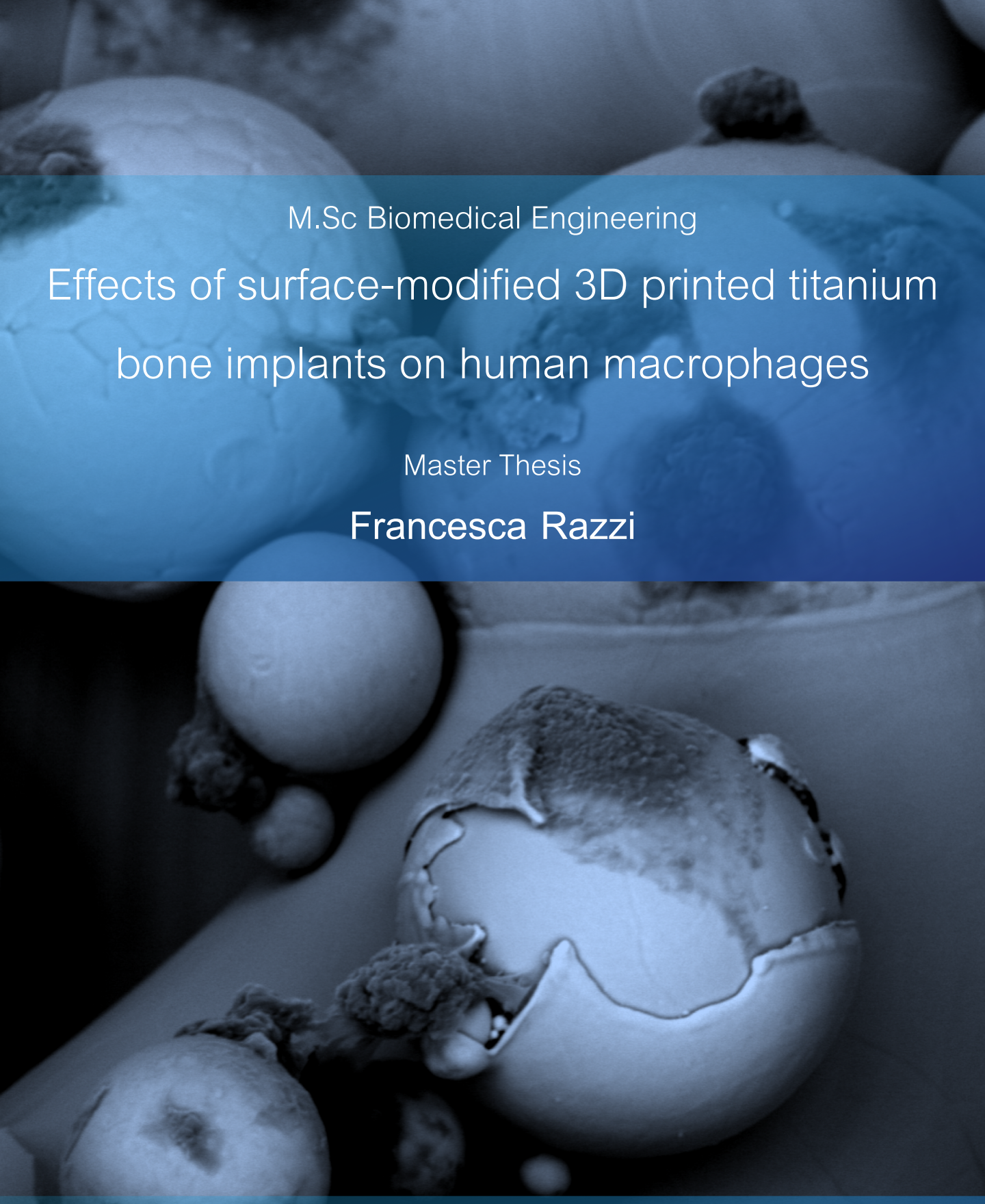

M.Sc Biomedical Engineering

Effects of surface-modified 3D printed titanium bone implants on human macrophages

Master Thesis

Francesca Razzi

Supervisors:

Dr. Ir. E. Lidy Fratila-Apachitei

Dr. Ir. Eric Farrell

Prof. Dr. A. Amir Zadpoor

TU Delft

Erasmus MC
University Medical Center Rotterdam

Effects of surface-modified 3D printed titanium bone implants on human macrophages

By

Francesca Razzi (4614453)

In partial fulfilment of the requirements for the degree of

Master of Science

In Biomedical Engineering

At the Delft University of Technology,

To be defended publicly on Tuesday August 28, 2018 at 15:00 PM

Supervisors:

Dr. ir. E.L. Fratila-Apachitei

Dr. ir. E. Farrell

Dr. ir. A.A. Zadpoor

Biomaterials and Tissue Biomechanics Section

Biomechanical Engineering Department

Faculty of Mechanical, Maritime and Materials Engineering

Delft University of Technology

Summary

Background. Titanium orthopaedic biomaterials to replace degenerated joint surfaces, improve bone regeneration and fixation are studied and used worldwide. However, not always biomaterial implantation is successful, and the main causes of implant failure remain implant associated infections (IAI) and poor osseointegration. Additive manufacturing and surface modification of titanium implants are promising strategies in order to develop bone implants able to enhance bone formation at material interface while reducing the risk of IAI. New bone formation at the implant site is an inflammation-driven process, resulting from paracrine signalling and factors released by inflammatory cells recruited on the biomaterial surface after implantation. Among the inflammatory cells involved, macrophages play a crucial role in regulating subsequent bone formation by secreting a wide range of pro-, anti-inflammatory and tissue repair-related factors. Therefore, in this study, human macrophage response to surface-modified 3D printed Ti-6Al-4V implants was investigated.

Methods. The 3D printed Ti-6Al-4V implants were modified by plasma electrolytic oxidation (PEO), during which an oxide layer containing electrolyte components was produced on implant surfaces. In order to provide an antimicrobial activity, silver nano-particles (Ag NPs) were also incorporated into the surface during the PEO process. Surface morphology and chemical composition were analysed by SEM. Human macrophages from different donors were cultured in the presence of implants in a transwell culture or directly on the implant surface for 4 days. Macrophage morphology and viability were assessed with scanning electron microscopy and fluorescence microscopy. Cell secreted factors were analysed by ELISA assay and gene expression analysis was performed. Human mesenchymal stem cell (hMSC) response in terms of morphology and viability was also evaluated after 4 days of culture. Finally, migration of MSCs in the presence of macrophage-conditioned medium (MCM) was investigated.

Results and Conclusions. PEO modification of 3D printed Ti-6Al-4V implants resulted in a TiO_2 layer containing electrolyte components (Ca, P and Ag NPs) and interconnected porosity. The ion release from PEO-treated surfaces did not have an effect on human macrophage polarization, while when cells were cultured directly on the implants, they secreted and expressed different amount of pro- and anti-inflammatory factors. Not treated surfaces up-regulated macrophage pro-inflammatory cytokines compared to PEO surfaces. PEO surfaces containing Ag NPs were cytotoxic for human macrophages but not for hMSCs, suggesting that macrophages are more sensitive to Ag NPs cytotoxic mechanisms. PEO-treated surfaces are promising in reducing the macrophage pro-inflammatory response and they are good candidates for the development of osteoimmunomodulatory implants. Nevertheless, also macrophages cultured on 3D printed not treated surfaces expressed anti-inflammatory and tissue repair-related factors, suggesting that either implant geometry achieved by additive manufacturing and surface biofunctionalization may have beneficial impact on promoting macrophage-mediated osteogenesis around the implant.

Acknowledgements

I would like to thank Dr. ir. Lidy Fratila-Apachitei from TU Delft for having given me the opportunity to work at this challenging but extremely stimulating research project at the Biomechanical Engineering Department. She has provided me with tight and well appreciated guidance during all the meetings we had in the whole course of the project.

I am also deeply grateful to Dr. ir. Eric Farrell from Erasmus MC, who I admire as a great professional and who put his wisdom and knowledge in his field at my disposal. He guided me along these 9 months of research and made me grow a lot both as a researcher and as a professional. I want to thank Eric also for giving me the opportunity to work in his extraordinary research group, I feel really lucky to have been part of the team.

Special thanks go to Niamh, whose unlimited patience have helped me enormously during the most challenging parts of my experiments. Moreover, Niamh's terrific enthusiasm and optimism was always capable to take the best out of myself, pushing me to overcome my limits, even during the toughest phases of my work.

Thanks a lot also to all my colleagues from Erasmus MC , not only for the precious suggestions they were always open to give me, but most of all for the great time spent with them in the lab enjoying doing research, and also having lot of fun in and outside the office.

Of course, I am immensely grateful to my family, for all the love and the support they give me in everything I do.

Thanks to Nicola, my boyfriend and my supporter number one, for simply being the way he is.

Thanks a lot to Livia, for having been always by my side from day one in Delft till the end. Finally, thanks to all my other "Delftian" friends who contributed filling these two years with some of the most beautiful moments of my entire life.

Table of contents

1. Introduction

Orthopaedic bone implants are extensively researched and used to replace degenerated natural joint surfaces or to repair large bone defects. A biomaterial must have the capability to exist in contact with living tissues in the human body without harming them, ensuring tissue integration while reducing the risk of infections and release of debris [1]. Different metals and metal alloys can be used for implantable biomedical devices in orthopaedics. Titanium and its alloys are preferred due to their strength, lower modulus relative to other metals and very good corrosion resistance [2]. However, although the success rate in total joint replacement surgeries is very high, the main limitations and the main problems are caused by implant associated infections (IAI), implant aseptic loosening and poor osseointegration [2,3]. Furthermore, titanium has been associated with release of ions, induction of allergies and poor bone in-growth [3].

In order to reduce the risk of implant failure, a promising strategy is the optimization of the 3D structure of scaffolds by changing implant porosity and pore size. Recent studies have shown that implant geometry, especially porosity of the structure, plays a crucial role in influencing bone-forming cell behaviour, promoting implant osseointegration [4,5]. For these reasons, in the recent years, additive manufacturing (AM) techniques to create bone implants have gained attention due to their capability to achieve different desirable implant functionalities at the same time, namely customizable 3D design (shape, size), intrinsic roughness and desired and controlled macroporosity [6]. Such implant properties have been shown to influence cell behaviour in terms of adhesion and bone formation, due to an increased surface roughness and surface area [7]. On the other hand, an increased implant surface area resulting from an increased porous structure, may lead to an increased microbial adhesion after implantation [8]. Thus, anti-microbial surfaces are required for these implants. Such property can be achieved by incorporating anti-microbial elements into titanium surfaces such as silver (Ag), zinc (Zn) or copper (Cu) [9–11]. Furthermore, host response at a cellular level can be manipulated by altering biomaterial surface properties such as chemical composition, wettability or topography. This can be achieved by applying different surface treatments which have the capability to control surface parameters and to create micro-environmental cues influencing immune and bone-forming cells [12].

New bone formation at the implant site after surgery is an inflammation-driven process. Insertion of an implant in the body is always followed by a host immune response, during which a cascade of events leads to the migration of cells of the innate immune system to the implant surface [13]. The main stages leading to tissue formation after biomaterial implantation include initial hemostasis, inflammation, tissue regeneration and tissue remodelling (**Figure 1**).

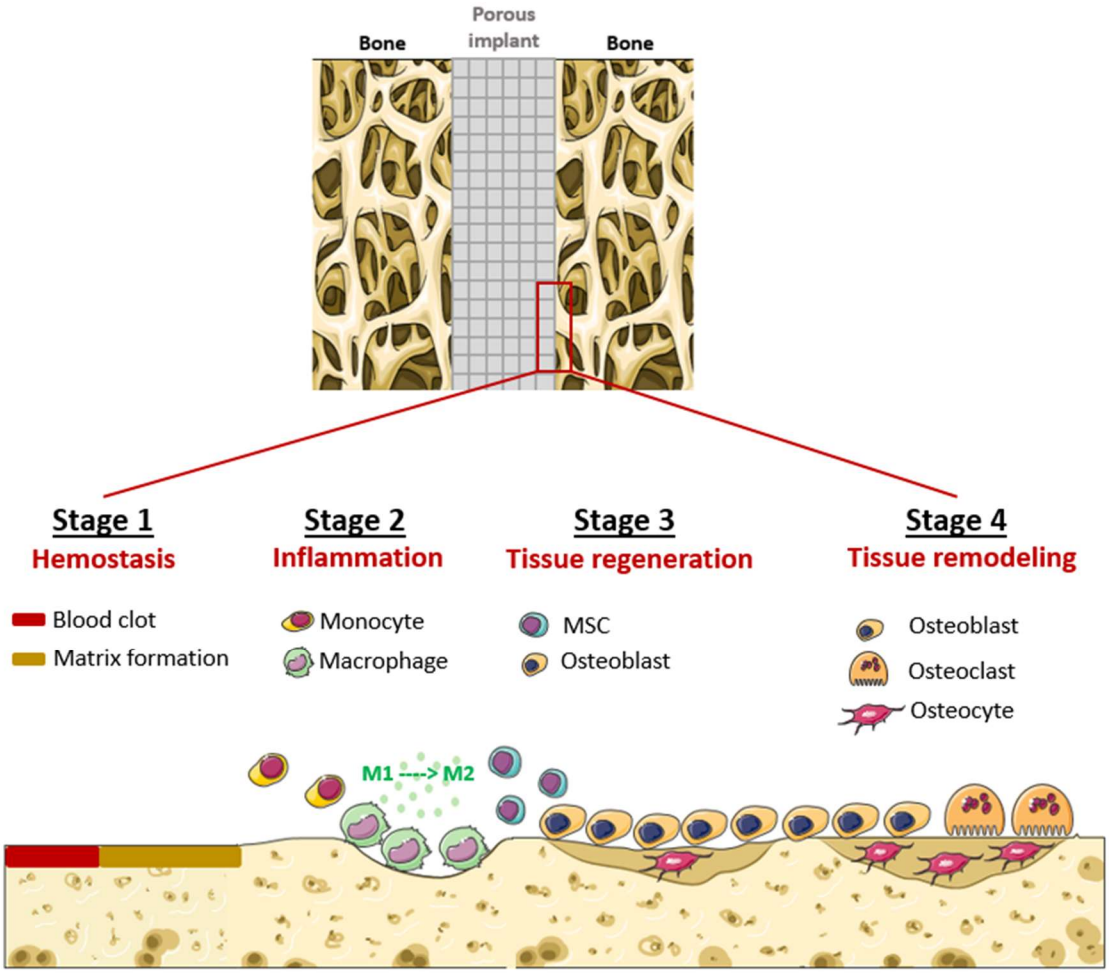

Figure 1*:* Stages of tissue repair after bone biomaterial implantation. During hemostasis, proteins adhere to the implant surface and a blood clot is formed. During the second stage, inflammatory cells are recruited to the implant site and macrophages secrete cytokines which promote the recruitment of bone forming cells, present at the implant surface during the tissue regeneration phase (stage 3). In the last stage, osteoblasts and osteoclasts orchestrate the formation and remodelling of new bone.

During the inflammation stage, inflammatory cells such as neutrophils, mast cells and peripheral blood monocytes, macrophage precursors, are recruited to the implant site [14]. Among these cells, macrophages play a crucial role affecting both inflammation and the new tissue formation phase through secretion of a wide spectrum of pro-, anti-inflammatory and tissue repair-related factors [15]. Macrophage activation is a continuum, meaning that such cells exist *in vivo* in a wide variety of polarization states occupying different positions in a continuous spectrum [16], where we can distinguish between three fundamental macrophage states:

- Classically activated (pro-inflammatory) macrophage (M1);
- Alternative activated (anti-inflammatory) macrophage (M2);
- Unstimulated or resting macrophage (M0).

Macrophage activation can be classified by different factors such as cytokine release, surface receptor expression and activity of reactive molecules, summarized in **Figure 2**. M1 macrophage secretes pro-inflammatory cytokines and inhibits anti-inflammatory cytokines. Its function is to kill intracellular pathogens mainly by phagocytosis and it has antimicrobial properties [17]. On the other hand, M2 macrophage can be further divided into three different subtypes, namely M2a, M2b and M2c. It secretes factors which dampen the inflammation and it has an important roles in wound healing [17,18].

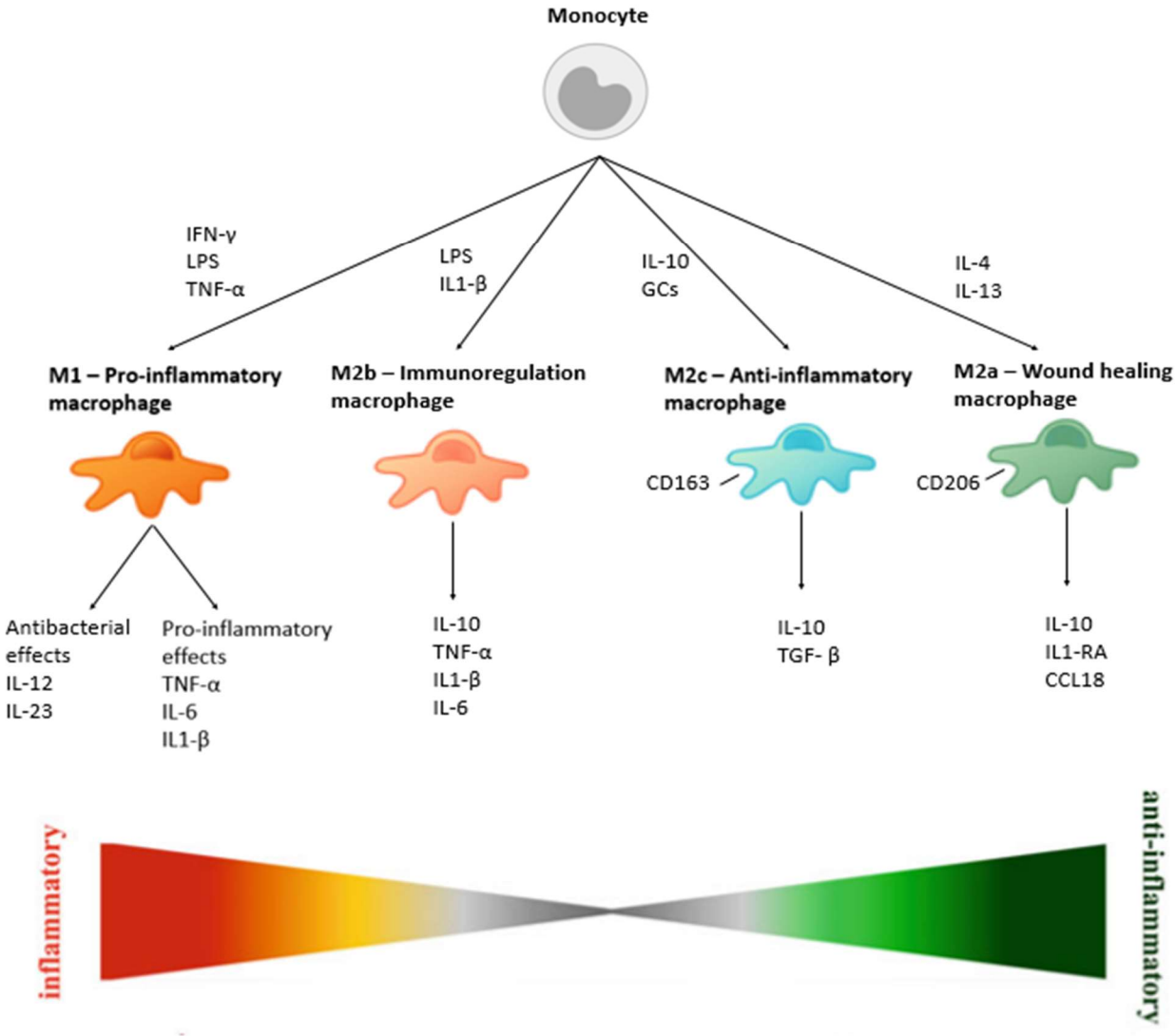

Figure 2: Inducers and factors secreted by macrophage phenotypes. Under the influence of different inducers, macrophages can switch into different phenotypes M1, M2 (M2a, M2b, M2c). Each phenotype has a specific surface markers and different functions.

During the early stage of inflammation, around 24 hours after surgery, an initial expression of pro-inflammatory cytokines is required in order to trigger the immune system response. However, a prolonged expression of these cytokines can eventually lead to tissue damage and fibrous encapsulation of the biomaterial [19]. On the other hand, a switch towards a M2 macrophage phenotype has been shown to regulate new bone formation by releasing osteogenic cytokines [12] and by recruiting mesenchymal stem cells

(MSCs). MSCs have a key role in tissue formation because of their capacity to differentiate into many cell types such as bone, cartilage and adipose cells [20]. For these reasons, the success of an implantable medical device is considered to be dependent on the fine balance between M1 and M2 macrophages around the implant, able to stimulate the subsequent tissue regeneration. In the case of bone implants, this concept is known as osteoimmunomodulation, and it attracted increased research interest lately [12,21].

While the effect of modified titanium surfaces on somatic and stem cells, relevant for tissue regeneration and remodelling phases, has been extensively researched [22–24], the effect on immune cells, including macrophages, is relatively less studied and therefore still not completely understood. Nevertheless, due to its key role in inflammation and wound healing, understanding the macrophage response to titanium surfaces represents a rational step forward for the development of a new generation of osteoimmunomodulatory bone implants.

In this research, human macrophage response to biofunctionalized 3D printed Ti-6Al-4V surfaces was investigated. Biofunctionalization of the 3D printed porous implants was achieved by plasma electrolytic oxidation (PEO) with the aim to generate surfaces that can simultaneously promote osseointegration and prevent IAI. During PEO process, a porous oxide layer is generated onto titanium substrate and electrolyte elements are incorporated in it altering the implant surface chemical composition and enhancing its biocompatibility [24]. In addition to this, surface antibacterial properties can be enhanced by incorporating antibacterial metal elements into the oxide layer during the treatment, inhibiting initial microbial adhesion and biofilm formation. Therefore, surface oxide layers with interconnected submicron porosity incorporating Ca and P species as well as Ag nanoparticles (Ag NPs) from the electrolyte were produced. These surfaces showed previously enhanced antimicrobial activity against methicillin-resistant *Staphylococcus aureus* MRSA [9].

In the present study, after having synthesized and characterized the 3D printed Ti-6Al-4V surfaces, the effects of such implants on the morphology, viability and polarization of human macrophages were investigated by scanning electron microscopy, fluorescence microscopy and specific protein and gene expression assays. Cells from different donors were included to evaluate donor variability. In parallel, viability of human MSCs was assessed on the same surfaces and compared to human macrophages. Finally, the effect of macrophage-conditioned medium (MCM) on hMSCs migration was evaluated. The research outline is shown in **Figure 3.**

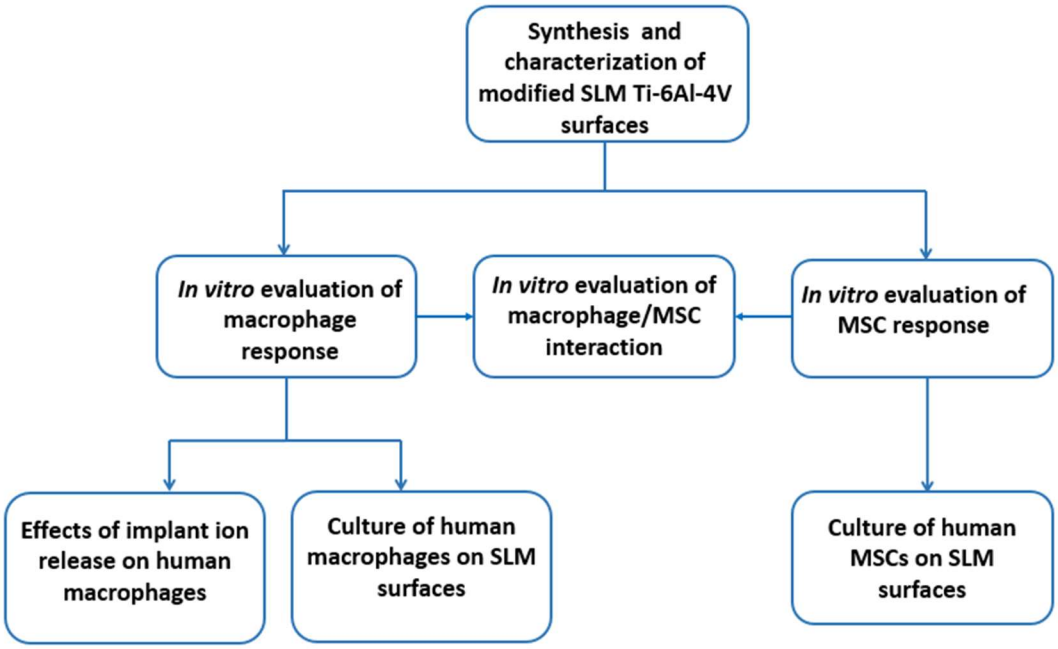

Figure 3: Schematic representation of the research outline.

2. Materials and Methods

2.1 Ti-6Al-4V implants

The Ti-6Al-4V implants were previously designed with interconnected pores in order to increase the surface area enabling bone ingrowth and implant fixation [9]. The pore size did not exceed 300 μm since this size has been shown to be optimal for bone regeneration [25,26].The dimensions of the implants were 40 mm in length and 0.5 mm in diameter (**Figure 4**). Implants were manufactured by selective laser melting (SLM) at the Additive Manufacturing Lab (TU Delft, Delft, The Netherlands). A SLM device (SLM-125, Realizer, Borchem, Germany) and medical-grade (ELI, grade 23) Ti-6Al-4V powder (AP&C, Boisbriand, Quebec, Canada) with spherical particles morphology and sizes between 10 μm and 45 μm were used.

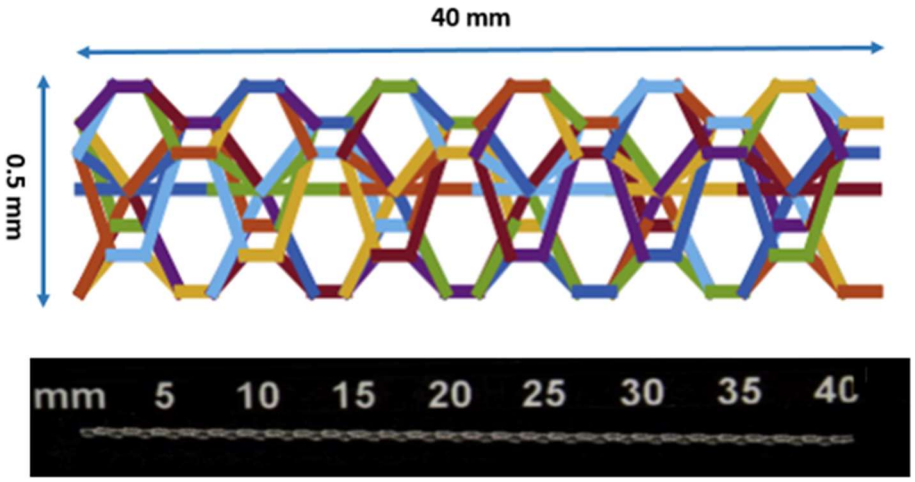

Figure 4: Design and SEM image of the 3D printed Ti-6Al-4V implant used in the study. Figure adapted from [9].

2.2 Plasma Electrolytic Oxidation (PEO)

Plasma Electrolytic Oxidation (PEO), also called micro-arc oxidation (MAO), is a high voltage electrochemical surface treatment process for generating firmly adherent porous oxide layers on certain metals. It is widely used to generate porous oxide layers (TiO_2) on Ti-based implant surfaces. This process enhances the Ti surface native oxide layer, resulting in increased roughness and porosity. During the process, according to the selected electrolyte, calcium (Ca) and phosphorus (P) species layer can be incorporated in the oxide layer, enhancing its biocompatibility and osseointegration ability [24]. In addition to this, surface antibacterial properties can be enhanced by incorporating antibacterial metal elements into the oxide layer during the treatment, inhibiting initial microbial adhesion and biofilm formation [9]. Furthermore, PEO not only modifies the morphology and chemical composition of the titanium oxide, but also surface energy and wettability are altered. As a consequence, cell/material interaction is increased [27]. The customized setup for PEO experiments is shown in **Figure 5**.

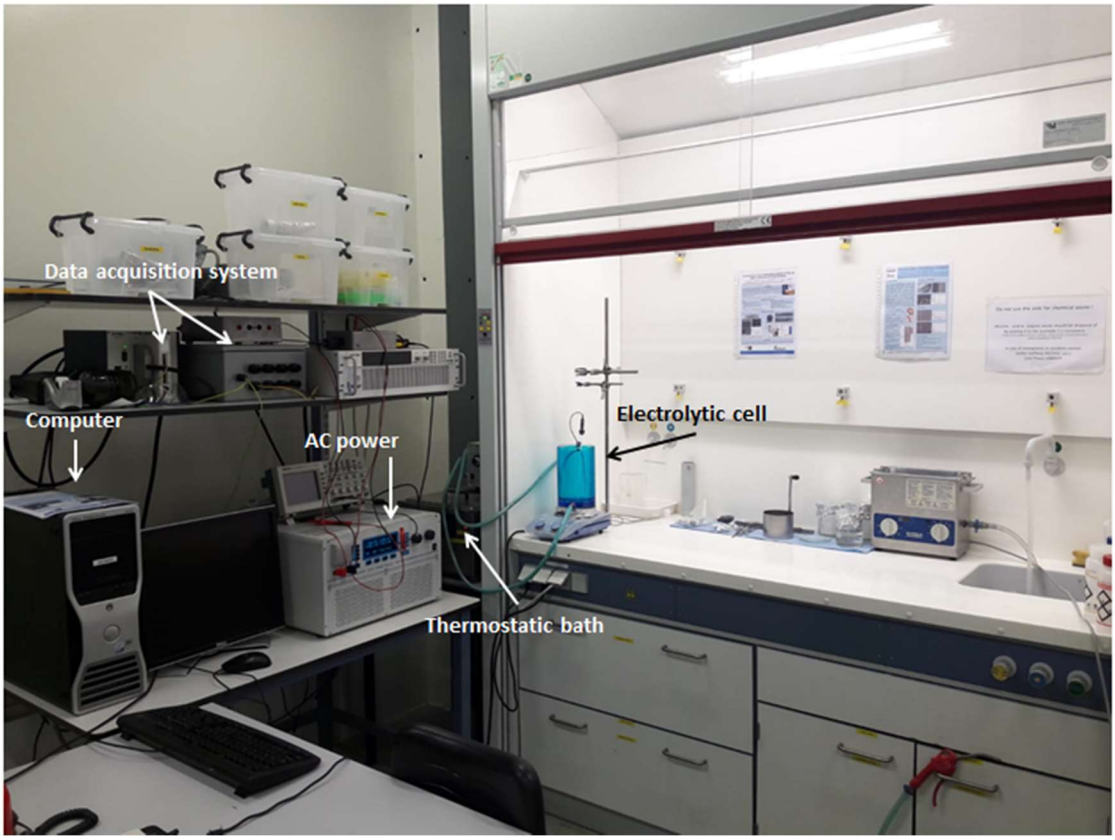

Figure 5: The custom-made PEO setup and the main components used at Surface Biofunctionalization Lab (TU Delft, Delft, The Netherlands). It consisted of an AC power supply (50Hz, type ACS 1500, ET Power Systems Ltd., UK), a computer interface connected with the AC power source through a data acquisition board (NI SCXI-1000, Austin, Texas, United States), a thermostatic bath (Thermo Haake V15, Karlsrhue, Germany) to maintain the electrolyte temperature during the process, and a cylindrical double walled electrolytic cell. The electrolytic cell presented two electrodes; a cylindrical cathode made of stainless steel was placed in the electrolytic cell while the Ti-6Al-4V implants represented the anode during the PEO process.

2.2.1 Electrolyte preparation

The PEO electrolyte was prepared with calcium acetate hydrate (CaA) (Sigma-Aldrich, St. Louis, USA) at a concentration of 24.0 g/L and calcium glycerophosphate (CaGly) (Dr. Paul Lohmann GmbH, Emmerthal, Germany) at a concentration of 4.2 g/L dissolved in distilled water. In order to generate TiO_2 surfaces with incorporation of silver nanoparticles (Ag NPs) (Sigma-Aldrich, St. Louis, USA), such nanoparticles with a size between 7 and 25 nm and with a spherical shape were dispersed in the above-mentioned PEO electrolyte at a concentration of 3.0 g/L. In order to achieve a homogeneous dispersion of Ag NPs, the electrolyte was placed in an ultrasonic bath for 3 minutes and it was stirred at 500 rpm for 5 minutes using a magnetic stirrer; this procedure was repeated twice. Finally, 800 mL of the electrolyte was added in the pre-cooled electrolytic cell (**Figure.A,B**). The type of surfaces produced and the PEO conditions used are included in **Table 1**.

Table 1: Surfaces produced by PEO, electrolyte composition and PEO conditions used.

Surfaces produced		Electrolyte composition			PEO conditions	
Abbreviation	**Content**	**CaA (g/L)**	**CaGly (g/L)**	**AgNP (g/L)**	**Current density**	**Oxidation time**
SLM NT	SLM Ti-6Al-4V implants, non-treated	-	-	-	-	-
SLM PEO	SLM Ti-6Al-4V implants oxidized by PEO	24.0	4.2	-	20 A/dm^2	300 s
SLM PEO + Ag	SLM Ti-6Al-4V implants oxidized by PEO + Ag NPs	24.0	4.2	3	20 A/dm^2	300 s

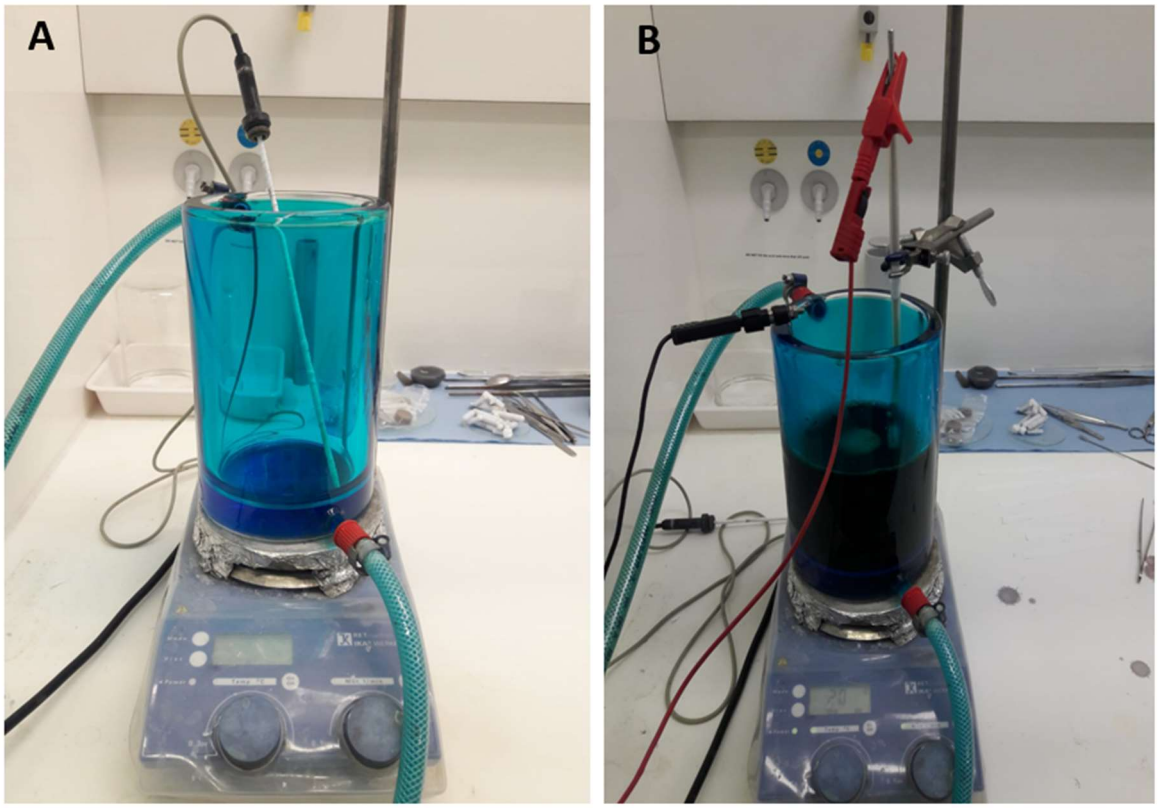

Figure 6: The double-walled electrolytic cell used in the study (A) containing 800 ml of electrolyte (B) during PEO process.

2.2.2 PEO-treated surface synthesis

The PEO procedure explained in this section was the same for both TiO_2 surfaces with and without incorporation of Ag NPs. The electrolyte was cooled to 5-8 °C by using the thermostatic bath that delivered cooling liquid composed of water and glycerol to the electrolytic cell through a pump system. In order to maintain the particle dispersion, the electrolyte was continuously stirred at 500 rpm. 3D printed Ti-6Al-4V implants were sonicated for 5 minutes in acetone, in 96% ethanol and finally in distilled water. The PEO

process was performed by immersing the implants in the electrolyte under a galvanostatic mode, using a constant current density of 20 A/dm^2 for 300 seconds, corresponding to around 390 mA applied to each implant. During this period, the voltage-time (V-t) curves were recorded at a sampling rate of 1 Hz. After the oxidation process, the Ti-6Al-4V samples were placed under running tap water for 2 minutes in order to remove the electrolyte before sterilization.

2.3 Implant surface characterization

Implant surface morphology was observed with SEM JSM-IT100 (JEOL, Tokyo, Japan), using an electron beam energy of 20kV and a working distance of 10 mm. In order to improve electrical conductivity, PEO-treated SLM implants were sputtered with a gold layer. Energy dispersive X-ray spectroscopy (EDS) was used to analyse the chemical composition of a specific surface spot. SEM imaging at different magnifications and EDS analysis were performed for all the experimental groups listed in **Table 1**.

2.4 *In vitro* evaluation of macrophage response

2.4.1 Effects of implant ion release on human macrophages

During the PEO process explained in section 2.2, electrolyte components are incorporated in the oxide layer. Such components may be released in the form of ions from the surface once implanted in the human body. As an example, titanium and silver ions have been previously shown to have toxic effects on different type of cells, both *in vitro* and *in vivo* [28,29]. Here, the effect of possible ion release from implant surfaces on human macrophage polarization was investigated. The entire experimental set up, described in details in the following sections, is shown in the schematic in **Figure 7**.

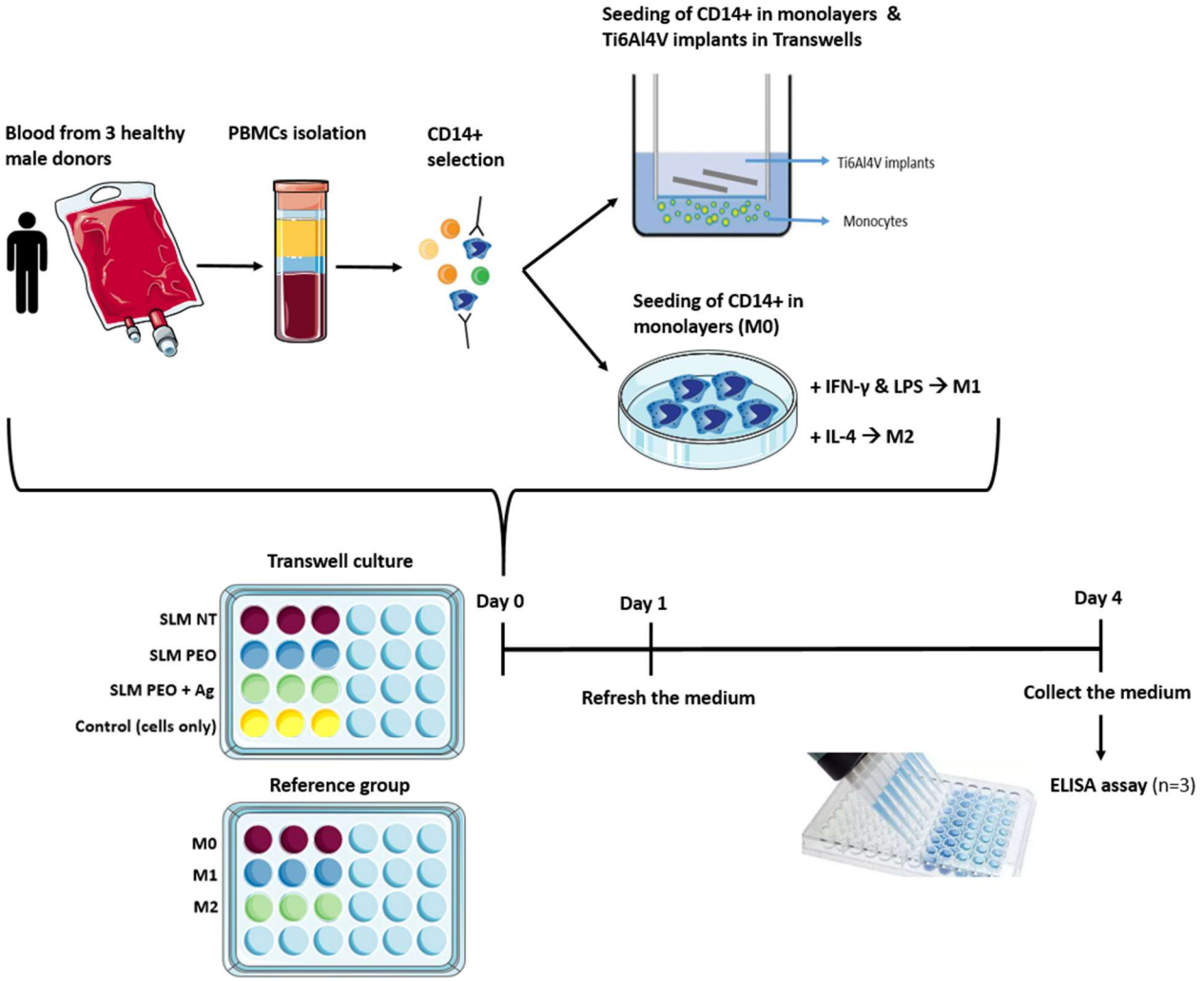

Figure 7: Schematic representation of the experiment performed in order to evaluate macrophage polarization in response to ion release from SLM implant surfaces. Peripheral blood mononuclear cells (PBMCs) were isolated from human buffy coats and monocytes (CD14+ cells) were selected by magnetic activation cell sorting (MACS) and seeded in monolayers in the presence of SLM in transwells. Each group was evaluated in triplicates (n=3). A negative control was included, composed of CD14+ cells only. CD14+ cells were also differentiated towards a M1 and M2 macrophage phenotype in order to generate a positive control for the experiment (n=3). After 4 days of culture, the concentration of the pro-inflammatory cytokines IL-6, TFN-α and the anti-inflammatory cytokine CCL18 was assessed performing an ELISA assay. The experiment was repeated three times using cells from different human blood donors (N=3).

2.4.1.1 Human peripheral blood monocytes isolation

Human peripheral blood mononuclear cells (PBMCs) were isolated from buffy coats from 3 different healthy male blood donors (Sanquin blood bank, Amsterdam, The Netherlands; contract number: NVT0053.01), using Ficoll (Ficoll-Paque™ PLUS, GE Healthcare, Little Chalfont, UK) density gradient separation followed by CD14+ magnetic-activated cell sorting microbeads (MACS; Miltenyi, Bergisch Gladbach, Germany). The buffy coat was transferred from the blood bag into a T175 flask, and was diluted with wash buffer composed of phosphate buffered saline (PBS; Gibco, ThermoFisher Scientific, Waltham, Massachusetts, USA) with 0,1% bovine serum albumin (BSA; Sigma Aldrich) until the end volume was approximately 240 ml. 30 ml of diluted

blood was slowly added to eight 50 ml tubes containing 15 ml Ficoll. The tubes were then centrifuged for 15 minutes of centrifugation at 1000 x g without brake, to perform density gradient separation [18,30].

Density gradient separation is based on the differential migration of cells during centrifugation. As a result, different layers are formed, which different blood cell types (**Figure 8**). The bottom red layer contains aggregated erythrocytes. Granulocytes are contained in the layer above the erythrocyte layer. Because of their lower density, peripheral blood mononuclear cells (PBMCs) are observed at the plasma/Ficoll interface [31].

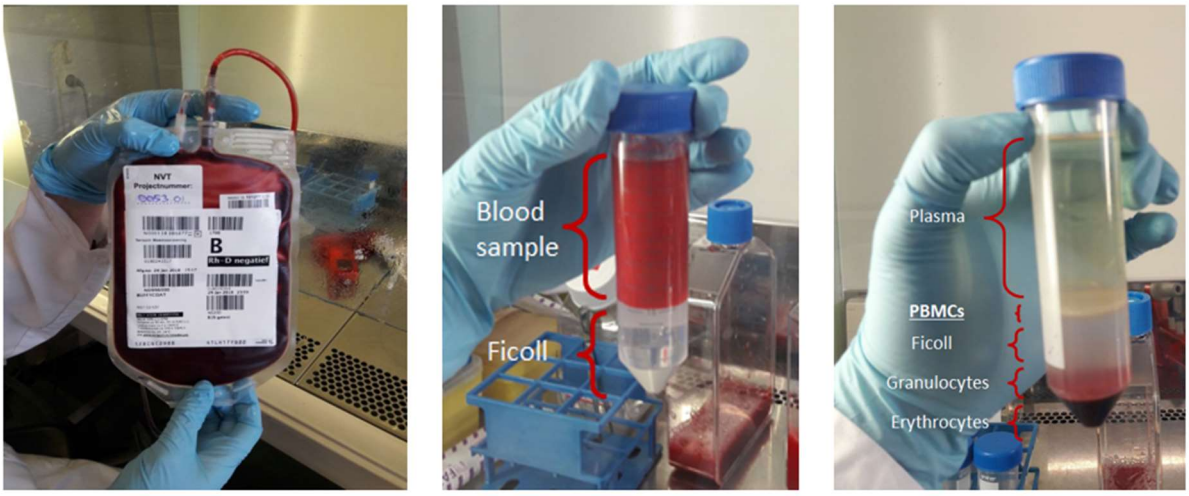

Figure 8: The image sequence shows first the blood bag obtained at the Sanquin blood bank Rotterdam. The second and the third images show the blood sample before centrifugation and after centrifugation, respectively.

The interphase band containing PBMCs was removed and washed in running buffer (PBS/0.5% BSA/2 mM EDTA (Invitrogen, Carlsbad, California, USA)). The cell suspension was then filtered through a 30 μm filter into a new 50 ml tube to remove any clumps. Monocytes are characterized by high levels of expression of the CD14 cell surface receptor, thus the obtained PBMC suspension were labelled with 100 μl of anti-CD14+ magnetic bead solution according to manufacturer instruction and incubated at 4 °C for 20 minutes in the dark in order to isolate only CD14+ cells. A magnetic field was applied to the cell suspension, and unlabelled cells passed through the column representing the negative fraction. Once the magnetic field was removed, the target cells were washed out as the enriched positive fraction, containing peripheral blood monocytes. Magnetic-activated cell sorting (MACS) principle is summarized in **Figure 9**.

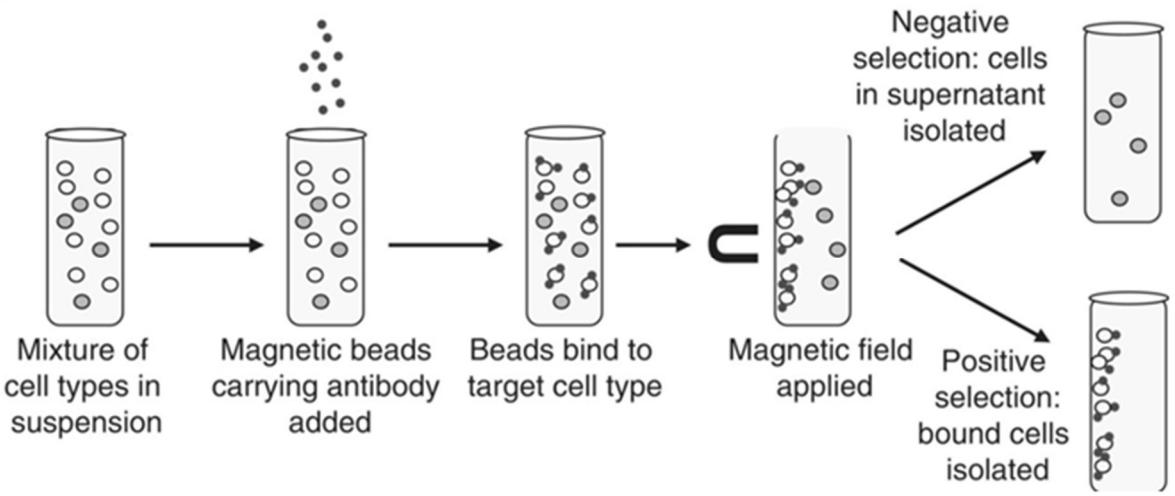

Figure 9: Magnetic Activated Cell Sorting (MACS) principle. After having isolated PBMCs, magnetic beads carrying antibody were added to the cell suspension and they bound to the CD14+ cells. After that, a magnetic field was applied in order to further isolate the target cell type, namely monocytes.

2.4.1.2 Transwell culture of human monocytes and titanium implants

To investigate the potential effect of ion release from the different treated titanium surfaces, monocytes were seeded in a 24-wells plate at a cell density of 500,000 cells/cm^2 to perform a co-culture with Ti-6Al-4V implants. Cells were cultured in 1 ml X-vivo medium (Lonza, Verviers, Belgium) supplemented with 20% heat-inactivated fetal bovine serum (FBS; Lonza), 50 μg/ml gentamycin (Gibco) and 1.5 μg/ml fungizone (Gibco). Such medium was previously shown to be suitable for this type of culture [18,30]. SLM NT, SLM PEO and SLM PEO + Ag implants (n = 6 per group) with a length of 0.5 cm were sterilized by autoclaving at 121 ^{O}C for 2 hours. Two implants of 0.5 cm in length were placed in transwell inserts of 5 μm pore size and placed in to each well, as shown in **Figure 10**. Three different experimental groups were investigated, namely SLM NT, SLM PEO and SLM PEO + Ag. A negative control was included in the experimental set up, composed of monocytes cultured in monolayers without the presence of implants in transwells. After 24 hours, medium was refreshed and after additional 72 hours, cell supernatant for each experimental group was harvested to investigate released cytokine concentration and images of monocytes in monolayers were taken by using light microscopy. The above-explained procedure was repeated for 3 different healthy male blood donors.

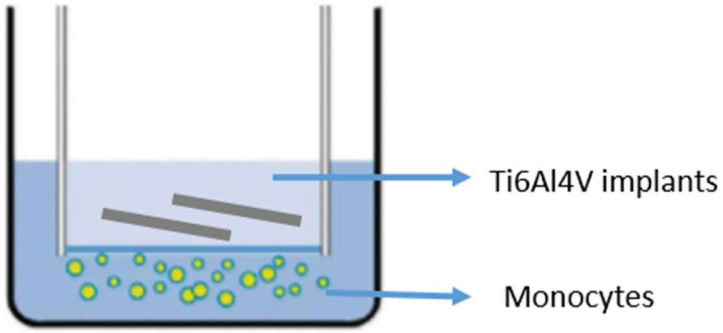

Figure 10: Transwell culture of human monocytes and titanium implants. Peripheral blood monocytes were cultured at a cell density of 500.000 cells/cm^2. Titanium implants were added in transwell inserts with a pore size of 5 μm.

2.4.1.3 Analysis of secreted pro- and anti-inflammatory factors

In order to evaluate the concentration of pro-inflammatory cytokines, namely IL-6 and TFN-α, and anti-inflammatory cytokine CCL18 in cell supernatant, commercially available enzyme-linked immunosorbent assay (ELISA) kits were used (DuoSet Development Kit; R&D Systems).

ELISA assay determines the presence of a molecule, in this case IL-6, TFN-α and CCL18, in cell culture supernatants. A "sandwich" ELISA method, capable of quantifying molecules between two layers of antibody (i.e. capture and detection antibody), was used according to manufacturer's instructions. A 96-well plate was prepared by adding 100 μl of capture antibody diluted in PBS to each well and incubated overnight at room temperature. The plate was washed with 200 μl of wash buffer composed of PBS containing 0.05% of Tween (Sigma Aldrich) and in order to block any non-specific binding sites on the well surface, 300 μl of reagent diluent (1% BSA, Fraction V, Protease free in PBS) was added to each well. After 1 hour, a seven-point standard curve was created in order to derive molecule concentration in the sample from known molecule concentration values and 100 μl of cell supernatant and standard was added to the plate. Samples were diluted in reagent diluent when values higher than standard curve range were expected. After 2 hours the plate was washed to remove unbound antigen and 100 μl of a specific detection antibody diluted in reagent diluent was added to each well. Finally, every 20 minutes, 100 μl of streptavidin-HRP solution, 100 μl of substrate solution (5 ml H_2O_2 and 5 ml tetramethylbenzidine) and 50 μl of stop solution (2N H_2SO_4) were added to each well. At the end of these procedures, the chemicals added were converted into colour depending on antigen concentration and finally the optical density of each well was read by VersaMax (Molecular Devices, San Jose, California, USA) at two wavelengths, namely 450 nm and 540 nm. The "sandwich" ELISA working principle is shown in **Figure 11**.

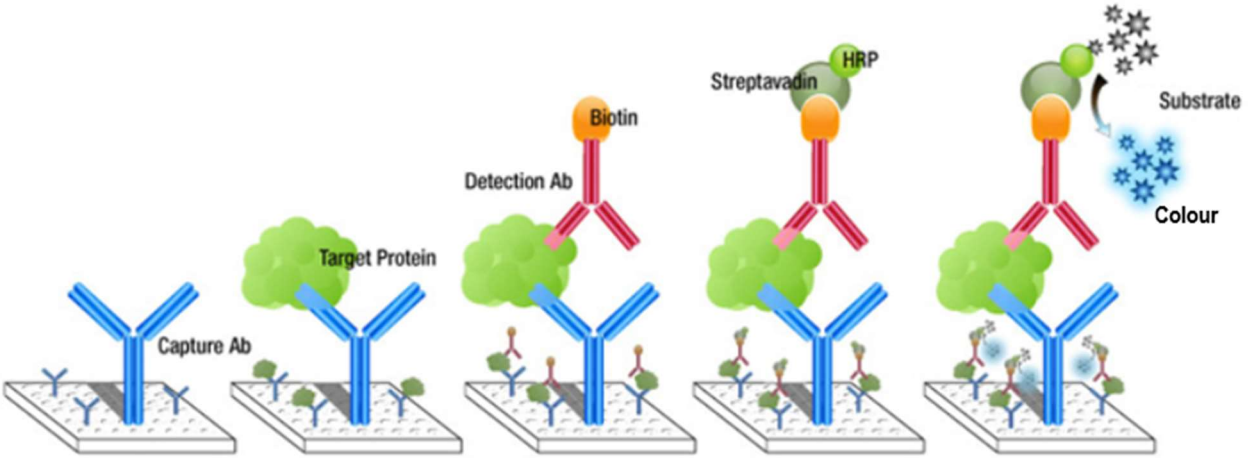

Figure 11: Working principle of the "sandwich" ELISA assay. A known quantity of capture antibody is added to a 96 well plate surface. The sample containing the target protein, which binds to the capture antibody, is applied to the plate. A detection antibody is added, which also binds to the target protein. Other enzyme-linked antibodies are applied. Finally, a chemical , which is converted by the enzyme into a colour, is added to the plate.

2.4.1.4 Human monocyte differentiation towards a M1/M2-like macrophage phenotype

In order to generate M1/M2 differentiated macrophages as a positive control for the transwell culture experiment, described in section 2.4.1.2, monocytes were seeded in a 24-well plate at a cell density of 500,000 cells/cm^2 in 1 ml X-vivo medium with supplement of 20% FBS, 50 µg/ml gentamycin and 1.5 µg/ml fungizone. In order to induce a differentiation of the human monocytes towards a macrophage M1 and M2 phenotype, 10 µg/ml Interferon-γ (IFN-γ; PeproTech, Rocky Hill, NJ, USA) & 100 µg/ml lipopolysaccharide (LPS), and 10 µg/ml Interleukin-4 (IL-4; PeproTech) were added, respectively. A negative control was included in the experimental set up, composed of non-stimulated monocytes (M0). After 24 hours, medium was refreshed and after an additional 72 hours M0, M1 and M2 supernatant was collected. Commercially available ELISA kits were used to determine the concentration of IL-6, TFN-α and CCL18 in the conditioned medium, following the procedure described in section 2.4.1.3 .

2.4.2 Culture of human macrophage on Ti-6Al-4V surfaces

In order to investigate the effects of different titanium implants on human macrophage polarization, cells were cultured directly on the surface. Cell protein secretion, gene expression and cell morphology were investigated to assess macrophage phenotype. The entire experimental set up, described in details in the following sections, is shown in the schematic in **Figure 12**.

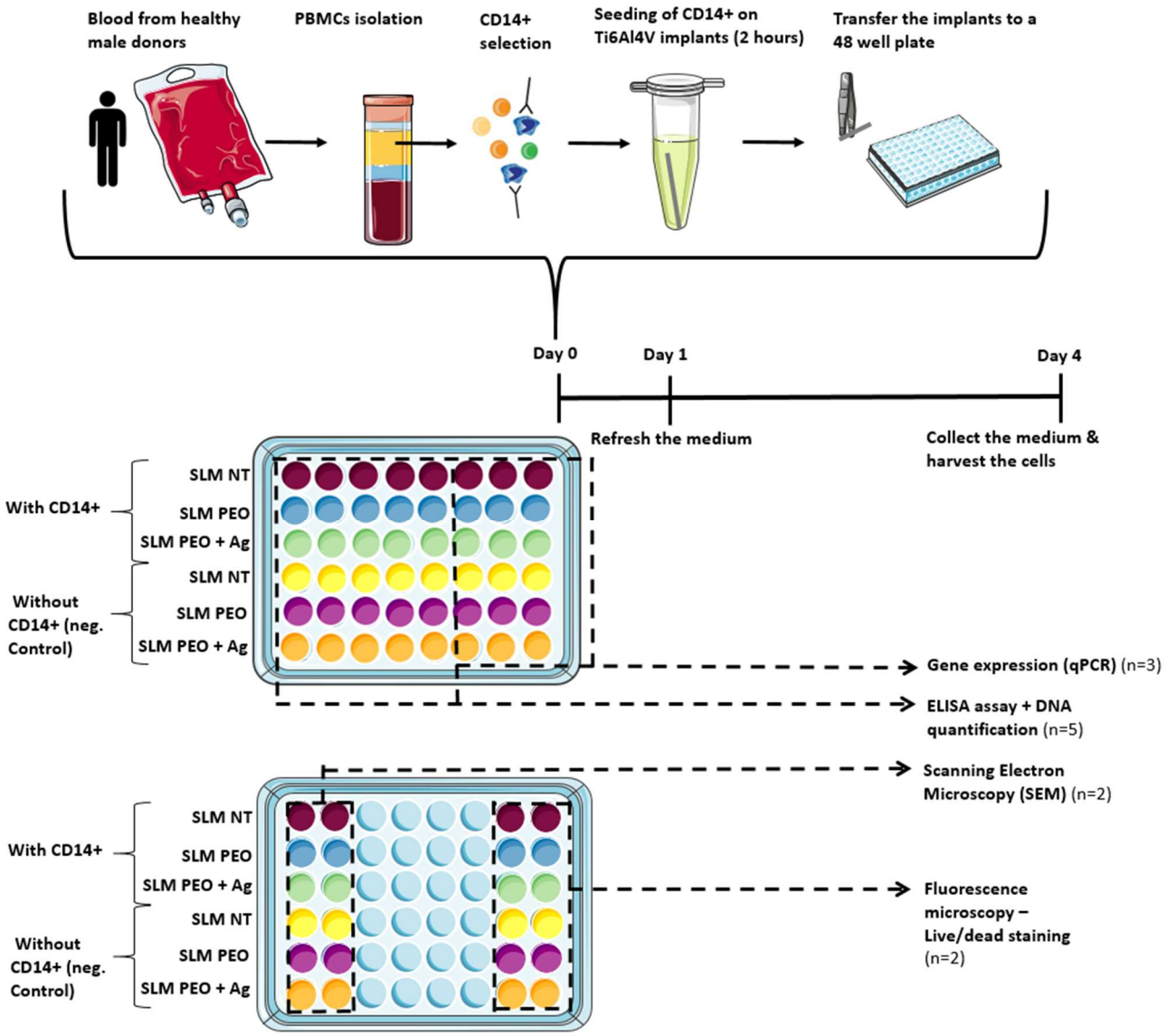

Figure 12: Schematic representation of the experiment performed in order to evaluate macrophage response when cultured on SLM Ti-6Al-4V implants. Peripheral blood mononuclear cells (PBMCs) were isolated from human buffy coats and monocytes (CD14+ cells) were selected by magnetic activation cell sorting (MACS) and seeded on SLM NT, SLM PEO and SLM PEO + Ag. After 2 hours, implants were transferred to a 48 well plate. For each experiment, a negative control was included, composed of SLM NT, SLM PEO and SLM PEO + Ag only, without cultured cells on the surface. The number of donors investigated for each experiment is reported in the text.

2.4.2.1 Human macrophage culture on implants

Human peripheral blood monocytes (CD14+) were isolated from buffy coats from healthy male blood donors, as explained in section 2.4.1.1. SLM NT, SLM PEO and SLM PEO + Ag implants with a length of 1 cm were sterilized by autoclaving at 121 ^{O}C for 2 hours. Each implant was placed in a 0.2 thin wall PCR reaction tube (BIOplastics, Landgraaf, The Netherlands) with 5 x 10^5 human peripheral blood monocytes in 100 µl of X-vivo medium supplemented with 20% FBS, 50 µg/ml gentamycin and 1.5 µg/ml fungizone. The samples were incubated at 37 ^{O}C and 5% CO_2, and turned 180^{O} every 30 minutes four times in order to enable homogeneous cell adhesion on implant surfaces. After 2 hours, implants were transferred to a 48-well plate in 400 µl of X-

Vivo medium using sterilized tweezers. A negative control was included in the experimental set up, composed of implants in X-vivo medium without adhered macrophages. The experimental set-up is shown in figure 15. After 24 hours of culture, the implants were transferred to a clean 48-well plate and the medium was refreshed in order to take into account only the cells adhered on the surface of the implants. 72 hours after refreshing, the medium was collected and macrophages were harvested in order to investigate cell morphology, viability, cytokine production and gene expression analysis. The assays performed, described in detail in the following sections, were repeated with cells from different donors in order to evaluate the experiment reproducibility.

2.4.2.2 Cell morphology

Human CD14+ cells from five different blood donors were cultured on the Ti-6Al-4V implants in order to investigate macrophage morphology using SEM after 4 days of culture. Adhered cells on the implants were first washed with PBS and then fixed in a solution of PBS with 4% paraformaldehyde (PFA) and 1% glutaraldehyde. Implants were kept at 4 ^{O}C for at least two hours. Implant dehydration was performed at room temperature, using a graded series of increasing ethanol concentrations, namely ethanol 50%, 70% and 96%. Finally, implants were allowed to dry overnight in a petri-dish. In order to take images with SEM, the samples were mounted on an aluminium stub with a carbon sticker on top and the stub with the implants was gold sputtered for 2 minutes. Both secondary electron mode (SEM) and backscattered modes (BEC) were used to image macrophages adhered to the different surfaces, but the backscattering mode was chosen as the best mode since with this it was easier to distinguish cells on implant surface due to their darker appearance. Different magnifications were used to take images, namely 100x, 200x, 500x, 1000x and 2000x magnification at one spot of the implant.

2.4.2.3 Cell viability

In order to assess viability of adhered macrophages on the implants after 4 days of culture a, live/dead staining of the cells was performed. Human CD14+ cells from two different blood donors were used. The assay is a two-colour fluorescence assay which determines the presence of live and dead cells simultaneously. It uses two different probes that measure intracellular esterase activity, namely calcein AM (CyQuant kit) in case on live cells, and plasma membrane integrity, measured by ethidium homodimer (EthD-1; CyQuant kit), in case of dead cells [32]. Calcein AM is retained within live cells, and it produces green fluorescence. This component is excited at 495 nm and emitted at 515 nm. On the other hand, EthD-1 can enter cells that have damaged membrane and it binds with nucleic acids producing a red fluorescence. It is excited at 495 nm and emitted at 635 nm. The implants with adhered cells in 48-well plate were washed 3 times in 0.9 % NaCl (saline) and were stained with 300 ul of a solution containing saline with 0.1% of Calcein AM and 0.15% of EthD-1. The samples were incubated at 37 ^{O}C for 40 minutes and rinsed 3 times in saline. The images were taken using a fluorescent microscopy using the FITC and the TRITC channels.

2.4.2.4 DNA quantification

In order to investigate the number of cells attached to the different surfaces and to normalize the cytokine secretion in the culture medium, DNA content was quantified for three different donors. Implants with adhered macrophages were stored at -20 ^{O}C in 0.5 ml tubes (Eppendorf, Hamburg, Germany). DNA content was assessed with a CYQUANT cell proliferation assay (Invitrogen, Carlsbad, California, USA). In order to lyse the adhered cells on the implants, 200 µl of papain digestion solution was added to each of the 0.5 ml tubes containing the samples previously stored at -20 ^{O}C. A negative control was included, composed of papain digestion solution only. Papain digestion solution was composed of papain buffer (0.2 M NaH2PO4 and 0.01 M EDTA.2H2O in MQ) with 0.01 M Cysteine HCL (Sigma Aldrich) and 250 µg/ml of papain. The tubes were incubated for 16 hours at 60 ^{O}C. 50 µl of samples and standard were pipetted into a 96-well plate in duplicate. 50 µl of heparin solution, 25 µl of ribonuclease type 3 solution and 0.375 ul of CYQUANT GR dye µl were added to each well. The CYQUANT GR dye was used since it shows considerable fluorescence enhancement when it binds to nucleic acids of the cells [33].Finally, the fluorescence was measured on a Spectramax Gemini (Molecular Devices) at 480 nm excitation and 520 nm emission.

2.4.2.5 Cytokine quantification

Commercially available ELISA kits (R&D Systems) were used according to manufacturer's instructions to determine the concentration of pro-inflammatory cytokine IL-6 and anti-inflammatory cytokine CCL18 in cell supernatant after 4 days of culture, as explained in section 2.4.1.3. After 4 days of macrophage culture on implants, cell supernatant was centrifuged for 5 minutes at 500 x g, aliquoted in 200 µl and stored at -80 ^{O}C for later cytokine quantification. During this procedure the different samples of each group were kept separately. The assay was performed for five different donors.

2.4.2.6 Gene expression analysis

After 4 days of culture, implants with adhered macrophages were added to a 1.5 ml tube containing 400 µl of TRIzol reagent (Thermo Fisher Scientific, Waltham, USA), and stored at -80 ^{O}C. In order to analyse the gene expression of macrophages cultured on the different surfaces, mRNA was isolated and cDNA synthesized from adhered cells prior to performing real-time polymerase chain reaction. Macrophages adhered to implants were collected in 400 µl TRIzol reagent after 4 days of culture, as described previously. TRIzol reagent is a solution composed of phenol, guanidine isothiocyanate and other components that which allow and facilitate RNA isolation [34]. Trizol reagent is used to disrupt the cells while maintaining RNA integrity by inhibition of RNase activity. After this sample homogenization step, 80 µl of chloroform was added and the samples were centrifuged for 20 minutes at 12000 x g and 4 ^{O}C to allow separation of sample phases. As shown in **Figure 13**, the aqueous upper layer contains RNA while the interphase and the bottom layer contain DNA and proteins respectively. RNA was isolated from the aqueous phase and 200 µl of isopropanol were added to allow RNA precipitation and the samples were centrifuged 10 minutes at 12,000 *x g*. Precipitated

RNA was washed twice with 400 µl of 75% ethanol to remove impurities and quantification of total extracted RNA was determines using a NanoDrop spectrophotometer (Thermo Fischer Scientific) at 260/280 nm.

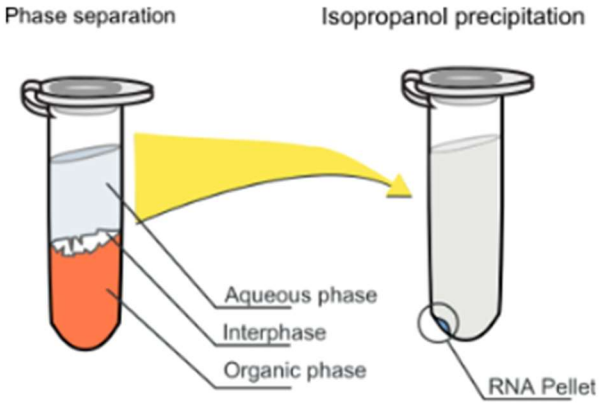

Figure 13: RNA isolation steps. On the left, the phase separation resulting from centrifugation. The upper phase (aqueous phase) contains RNA. On the right, precipitated RNA pellet after isopropanol precipitation.

After RNA quantification, complementary DNA (cDNA) was synthesized. cDNA is used as template for qPCR analysis since it is more stable than the corresponding RNA template and can be easily amplified during such analysis [35]. cDNA was synthesized using the RevertAid First Strand cDNA Synthesis Kit (Thermo Fischer Scientific). 110 ng of RNA previously isolated was incubated with 0.5 µl of Oligo-d(T)18 primer and 0.5 µL Random Hexamer primer and ddH_2O for 5 minutes at 70° C. After incubation, the tubes were chilled on ice for 5 minutes and the enzyme mix containing reaction buffer, dNTPs, Ribolock inhibitor and RevertAid M-MulV Reverse Transcriptase was added. A control without Reverse Transcriptase and one containing only ddH_2O were also included. Next, the tubes were incubated for 5 minutes at 25°C, 60 minutes at 42°C and 10 minutes at 70°C. After cooling to 12°C, 100 µl ddH_2O was added to dilute the cDNA of each sample. qPCR was performed to quantify macrophages gene expression. Gene expression in a cell can be measured by the number of copies of an RNA transcript of that gene present in a sample. qPCR is a technique used to monitor the amplification of a targeted nucleic acid, in this case the cDNA, as it occurs, allowing the determination of its starting concentration [35]. In order to detect the PCR products accumulation, the qPCR contains a fluorophore which binds to DNA and emits increasing fluorescence as the quantity of target amplification increases. Such fluorophores can be a TaqMan probe or SYBR Green dye. For each gene a mastermix was prepared, composed of 5.0 µl of 2x qPCR mastermix (Sybr green or taqman) and 0.5 µl of primer mix. 5.5 µl of mastermix and 4.5 µl of cDNA were added to a pre-cooled PCR plate and gene expression was quantified using a Bio-Rad CFX96 Real-Time PCR Detection system (Bio-Rad, Hercules, CA, USA). Glyceraldehyde-3-phosphate dehydrogenase (GAPDH) and hypoxanthine phosphoribosyltransferase 1 (HPRT1) were tested as housekeeper. GAPDH was used as housekeeper because it was found the most stable. In order to assess macrophage phenotype when cultured on titanium surfaces, IL-6, TNF-α and IL1-β were used as genes

encoding pro-inflammatory cytokines while IL1-RA, IL-10, CCL18, CD163 and CD206 were used as genes encoding anti-inflammatory cytokines. VEGF and TGF-β1 expression was also investigated, since these are factors involved in tissue repair and mostly secreted by M2 phenotype. The genes analysed are listed in **Table 2**.

Table 2: Macrophage cytokines, surface markers and growth factors investigated with qPCR.

Genes			
Pro-inflammatory (M1)	**Anti-inflammatory (M2)**		
Cytokines	**Cytokines**	**Surface markers**	**Growth factors**
IL1- β IL-6 TNF-α	IL1-RA IL-10 CCL18	CD163 CD206	TGF-β1 VEGF

The gene expression relative to GAPDH expression was determined by the $2^{-\Delta CT}$ formula, where $\Delta Ct = Ct_{sample} - Ct_{GAPDH}$. Gene expression analysis was performed for five different donors. All the primers used are listed in **Table 3**.

Table 3: Primers and probes used for qPCR analysis

Gene	**Fw**	**Rev**	**Probe**
IL-6	TCGAGCCCACCGGGAACGAA	GCAGGGAAGGCAGCAGGCAA	
IL1- β	CCCTAAACAGATGAAGTGCTCCTT	GTAGCTGGATGCCGCCAT	
TNF-α	GCCGCATCGCCGTCTCCTAC	AGCGCTGAGTCGGTCACCCT	
CCL18	GCACCATGGCCCTCTGCTCC	GGGCACTGGGGGCTGGTTTC	
IL1-RA	AACAGAAAGCAGGACAAGCG	CCTTCGTCAGGCATATTGGT	
CD206	TGGCCGTATGCCGGTCACTGTTA	ACTTGTGAGGTCACCGCCTTCCT	
CD163	GCGGGAGAGTGGAAGTGAAAG	GTTACAAATCACAGAGACCGCT	
IL-10	CCTGGAGGAGGTGATGCCCCA	GACGCGCCGTAGCCTCAGC	
TGF-β1	GTGACAGCAGGGATAACACACTG	CATGAATGGTGGCCAGGTC	ACATCAACGGGTTCACTACCGGC
VEGF	CTTGCCTTGCTGCTCTACC	CACACAGGATGGCTTGAAG	
HPRT1	TATGGACAGGACTGAACGTCTTG	CACACAGAGGGCTACAATGTG	AGATGTGATGAAGGAGATGGGAGG CCA
GAPDH	CAACGGATTTGGTCGTATTGGG	TGCCATGGGTGGAATCATATTGG	GGCGCCCCAACCAGCC

2.5 *In vitro* evaluation of human MSC response

2.5.1 Culture of human mesenchymal stem cells on Ti-6Al-4V surfaces

Pediatric mesenchymal stem cells (MSCs) were isolated from leftover material from patients undergoing alveolar bone graft surgery as previously described [36]. Cells were plated at approximately 2,300 cells/cm^2 in complete expansion medium (alpha-mem containing 10% fetal bovine serum (lot# 41Q204K, Gibco), 50 μg/ml gentamycin and 1.5 μg/ml fungizone supplemented with 25 μg/ml L-ascorbic acid 2-phosphate and 1 ng/ml fibroblast growth factor-2 (Instruchemie, Delfzijl, Netherlands) at 37°C and 5% carbon dioxide (CO_2) in a humidified atmosphere. Medium was replenished every 3-4 days until cells reached approximately 80-90%

confluency. The implants (n = 4/group) were cut with a length of 1 cm each and were sterilized at 121 ^{O}C for 2 hours by autoclaving. The seeding protocol used was the same as described in section 2.3.2.1. SLM NT, SLM PEO and SLM PEO + Ag were put in 0.2 PCR thin wall reaction tube with 1.5 x 10^5 hMSCs in 100 µl of α-MEM supplemented with 10 % FBS, 50 µg/ml gentamycin, 1.5 µg/ml fungizone , 1 ng/ml fibroblast growth factor 2 (FGF-2) and 10^{-4} M vitamin C. The samples were incubated at 37 ^{O}C and 5% CO_2, and turned 180^{O} every 30 minutes four times in order to enable homogeneous cell adhesion on implants surface. After 2 hours, implants were transferred to a 48-wells plate in 400 µl of culture medium using sterilized tweezers. The medium was refreshed after 24 hours and cell morphology and viability were assessed after additional 72 hours.

2.5.2 hMSC morphology

SEM was used to evaluate hMSCs morphology after 4 days of culture on the different titanium surfaces. Adhered cells were fixed and imaged with the same procedures as explained in section 2.4.2.2.

2.5.3 hMSC viability

SLM implant cytotoxicity for hMSCs was investigated by live/dead staining culturing cells from two different donors for 4 days. After 4 days of culture, a live/dead staining of the cells was performed as described in section 2.4.2.3.

2.6 *In vitro* evaluation of macrophage/MSC interaction

As explained previously, macrophages at implant interface secrete a wide range of factors that eventually recruit bone-forming cells, including MSCs. Here, the effect of the macrophages attached to the different SLM surfaces on migration of hMSCs was evaluated. The experimental set-up is shown in **Figure 14** and the experimental details are presented in the following sections.

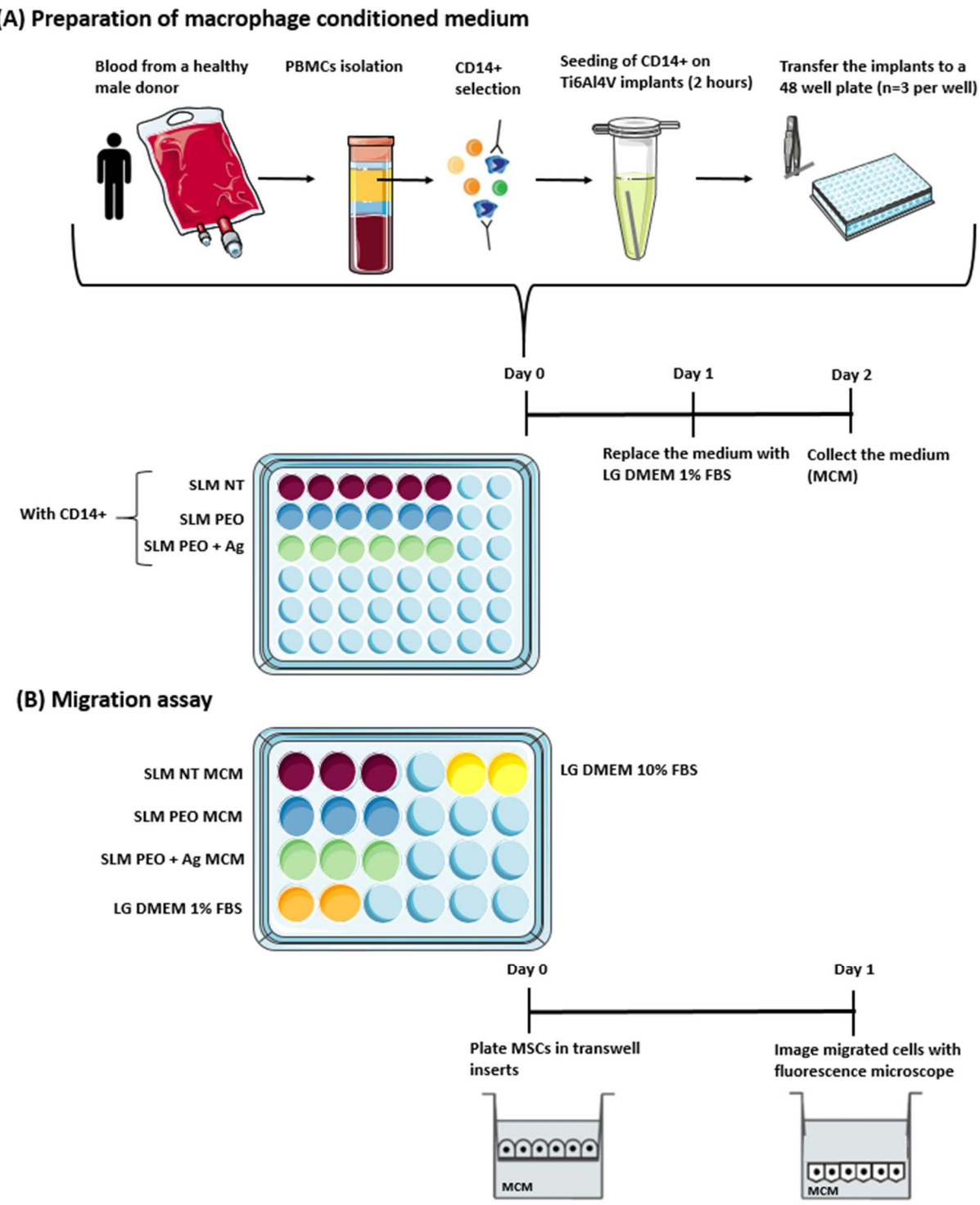

Figure 14: Schematic representation of the experiment performed in order to evaluate macrophage/MSC interaction. (A) Peripheral blood mononuclear cells (PBMCs) were isolated from human buffy coats and monocytes (CD14+ cells) were selected by magnetic activation cell sorting (MACS) and seeded on SLM NT, SLM PEO and SLM PEO + Ag. After 2 hours, implants were transferred to a 48 well plate (n=3 implants per well). After 1 day of culture, medium was replaced with LG DMEM with 1% FBS and after additional 24 hours the CM was collected. (B) Migration assay of MSC using MCM. MSCs were plated in transwell insert (n=3 per SLM implant group and n=2 per controls) and after 16 hours the number of migrated cells was evaluated with a fluorescence microscope.

2.6.1 Macrophage-condition medium (MCM) preparation

Human peripheral blood monocytes (CD14+) were isolated from one buffy coat from a healthy male blood donor, as explained in section 2.4.1.1 and the SLM implants were seeded according to the procedure previously explained (section 2.4.2.1). After 2 hours of incubation at 37°C and 5% CO_2, implants were transferred to a 48-well plate (n=3 implants per well) in 800 µl of X-Vivo medium supplemented with 20% FBS, 50 µg/ml gentamicin and 1.5 µg/ml fungizone. In order to generate MCM, after 24 hours of culture, the medium was replaced with the same volume of Low Glucose Dulbecco's Modified Eagle medium (LG DMEM; Gibco) with 1% FBS, a medium considered more suitable for MSC culture. After 24 hours, this medium was collected, spun down and cell supernatant was saved in aliquots and stored at -80°C. The implants with adhered macrophages were stored at -20°C for further DNA quantification analysis. In order to take into account the number of macrophages that conditioned the medium, a DNA assay was performed as explained in section 2.4.2.4. The condition medium was prepared using 50:50 LG DMEM with 1% FBS: MCM. The DNA contents per condition were summed and the values for all the conditions investigated (SLM NT, SLM PEO, SLM PEO + Ag) were averaged and defined as 50%. The MCM percentage to use in hMSC culture was adjusted for the DNA content per condition.

2.6.2 MCM effects on MSC migration

hMSCs were isolated and expanded according to the procedures explained in section 2.5.1. In order to perform a migration assay, 15,000 MSCs in 200 µl LG DMEM were added in transwell inserts with pore size of 8.0 µm (Fischer Scientific) and 600 µl of the previously generated MCM was added in the wells of a 24-well plate (n=3 wells per condition). Two medium controls were included, composed of LG DMEM with 1% FBS and LG DMEM with 10% only. After 16 hours of incubation at 37 °C and 5% CO_2, the medium was removed and the transwell inserts were washed twice with PBS. Adhered cells on the insert membrane were fixed with 4% formalin for 20 minutes and they were stained with 500 µl of DAPI staining solution for 4 minutes. The images of migrated cells through the insert membrane were taken using a fluorescent microscopy using the DAPI channel. The migrated cells were imaged at a magnification of 100X, and five images were taken for each insert membrane in order to have a reliable quantification of migrated cells.

2.7 Statistical analysis

Microsoft Excel 2013 and IBM SPSS 24.0 were used for calculations and statistical analysis. After testing normal distribution of values, linear mixed models followed by Bonferroni post-hoc correction were used to determine the statistical significance between different conditions. The different experimental groups, namely SLM NT, SLM PEO and SLM PEO + Ag were considered as fixed factors and donors as random factors. The correlated p-values are shown in the results. For the statistical tests, differences of the means were considered statistically significant when p value was lower than 0.05.

3. Results

3.1 Plasma Electrolytic Oxidation (PEO)

3.1.1 Voltage transients

During the PEO process, the anodizing voltage increased rapidly for around 10 seconds until dielectric breakdown occurred, leading to a decrease of the oxide layer resistance, with a consequent slowing down in voltage increase (**Figure 15**). From this stage onwards, since the current density is maintained, spark discharges were observed homogeneously along the surface. No differences were observed in the V-t response curves between samples in the electrolyte without AgNP and the electrolyte with AgNP at a concentration of 3.0 g/L.

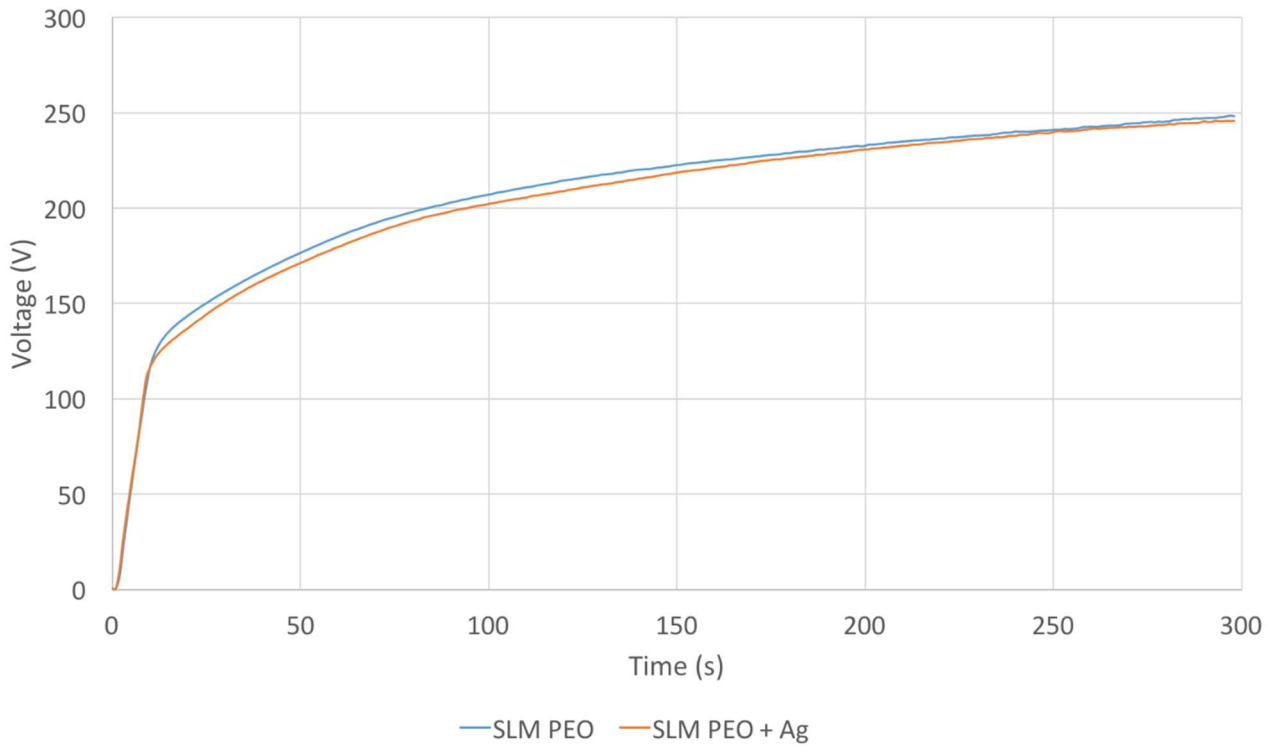

Figure 15: Voltage transients recorded during PEO process. No difference was observed in the V-t curves between the synthesis of SLM PEO (blue line) and SLM PEO + Ag (orange line) implants.

3.2 Implant surface characterization

3.2.1 Surface morphology of SLM implants

SLM NT implants presented a rough surface due to the presence of Ti-6Al-4V particles on the surface, partially melted during the additive manufacturing process (**Figure 16.A,B**). The PEO process modified significantly the surface topography, characterized by a uniformly distributed porous oxide layer and interconnected

porosity (**Figure 16.C,D**). The presence of Ag NPs in the oxide layer did not change the typical topography generated by PEO process (**Figure 16.E,F**).

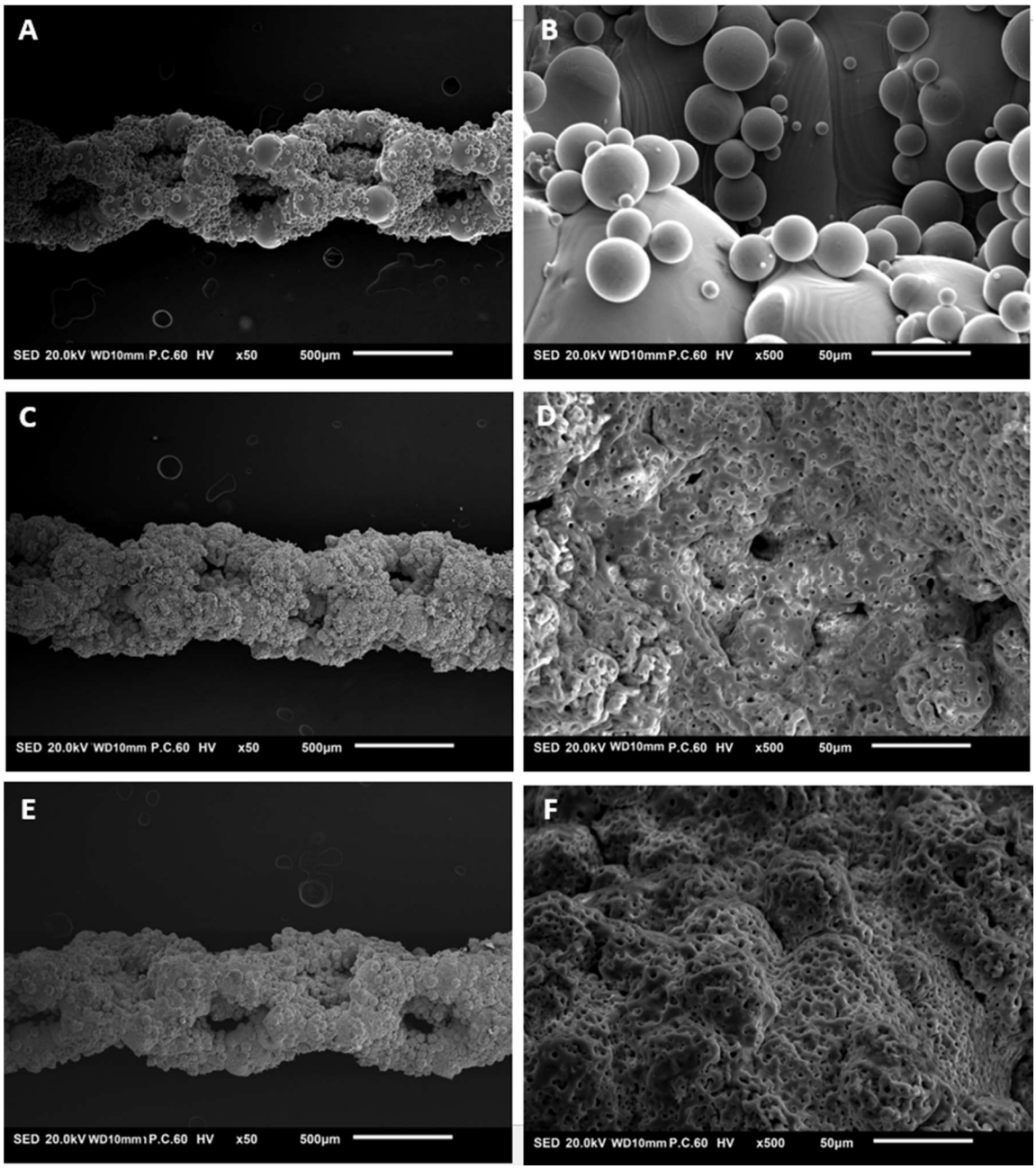

Figure 16: SEM images showing morphology of SLM implants at 50X and 500X magnification as revealed by SEM in secondary electron mode (SEM-SED). SLM NT surface (a,b) present a rough surface due to un-melted Ti-6Al-4V powder. PEO process produced an interconnected porous structure on implant surface due to the generation of the TiO_2 layer (c,d,e,f). No difference in morphology was observed between SLM PEO and SLM PEO + Ag groups.

3.2.2 Chemical composition of SLM implants

The surface chemical composition of SLM implants at different spots was examined by EDS analysis during SEM imaging. The chemical composition of the substrate material (SLM NT) is shown in **Figure 17.A,B**. After

PEO processing, electrolyte components (Ca and P) were incorporated into the surface (**Figure 17.C,D**). On SLM PEO + Ag implants, Ag NPs were found homogeneously distributed over the entire surface (**Figure 17.E**) and their presence was confirmed by the EDS analysis result in **Figure 17.F**.

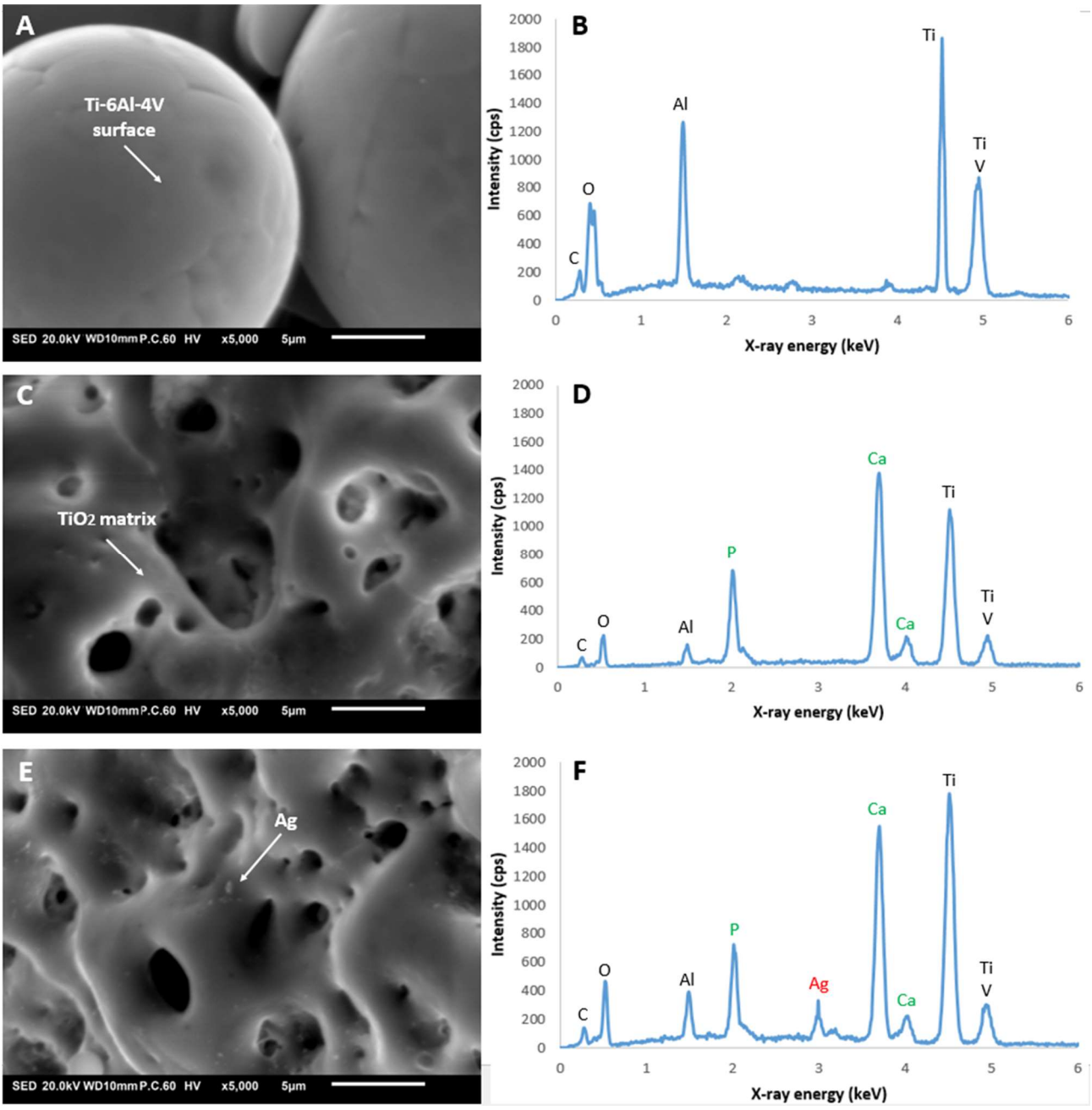

Figure 17: EDS analysis of SLM implants spots revealed the presence of C, O, Al, Ti and V on SLM NT surfaces (a,b). During PEO process, components of electrolyte (Ca and P) were incorporated into the TiO_2 matrix (c,d). Ag nanoparticle on SLM PEO + Ag surface was imaged with SEM (e) and EDS analysis revealed the presence of Ag on such surface (f).

3.3 *In vitro* evaluation of macrophage response

3.3.1 Human monocyte differentiation towards a M1/M2-like macrophage phenotype

In order to generate a positive control for macrophages with a M1/M2 phenotype, monocytes were differentiated with IFN-γ and LPS (M1) or IL-4 (M2) in monolayer culture in a different plate. Looking at the cells under light microscopy, their morphology can be assessed during culture. At day 1, cells from different experimental groups do not present any morphological differences whereas at day 4, cells induced towards M1 phenotype are more elongated compared to the M0 and M2 cells, that present a spherical shape (**Figure 18**).

After 4 days of culture, the concentration of the pro-inflammatory IL-6 and TNF-α and anti-inflammatory cytokine CCL18 in cell supernatant was investigated for three different donors by an ELISA assay. IL-6 and TNF-α concentrations were significantly higher in M1 phenotype compared to both M0 and M2 phenotype (**Figure 19**). Furthermore, IL-6 concentration in M0 supernatant was significantly higher compared to IL-6 concentration secreted by M2 cells. Alternatively activated macrophages (M2) up-regulated significantly CCL18 secretion compared to the other two phenotypes, while between M0 and M1 group it was not found any significant difference in CCL18 concentration. The results are listed in **Table 4**.

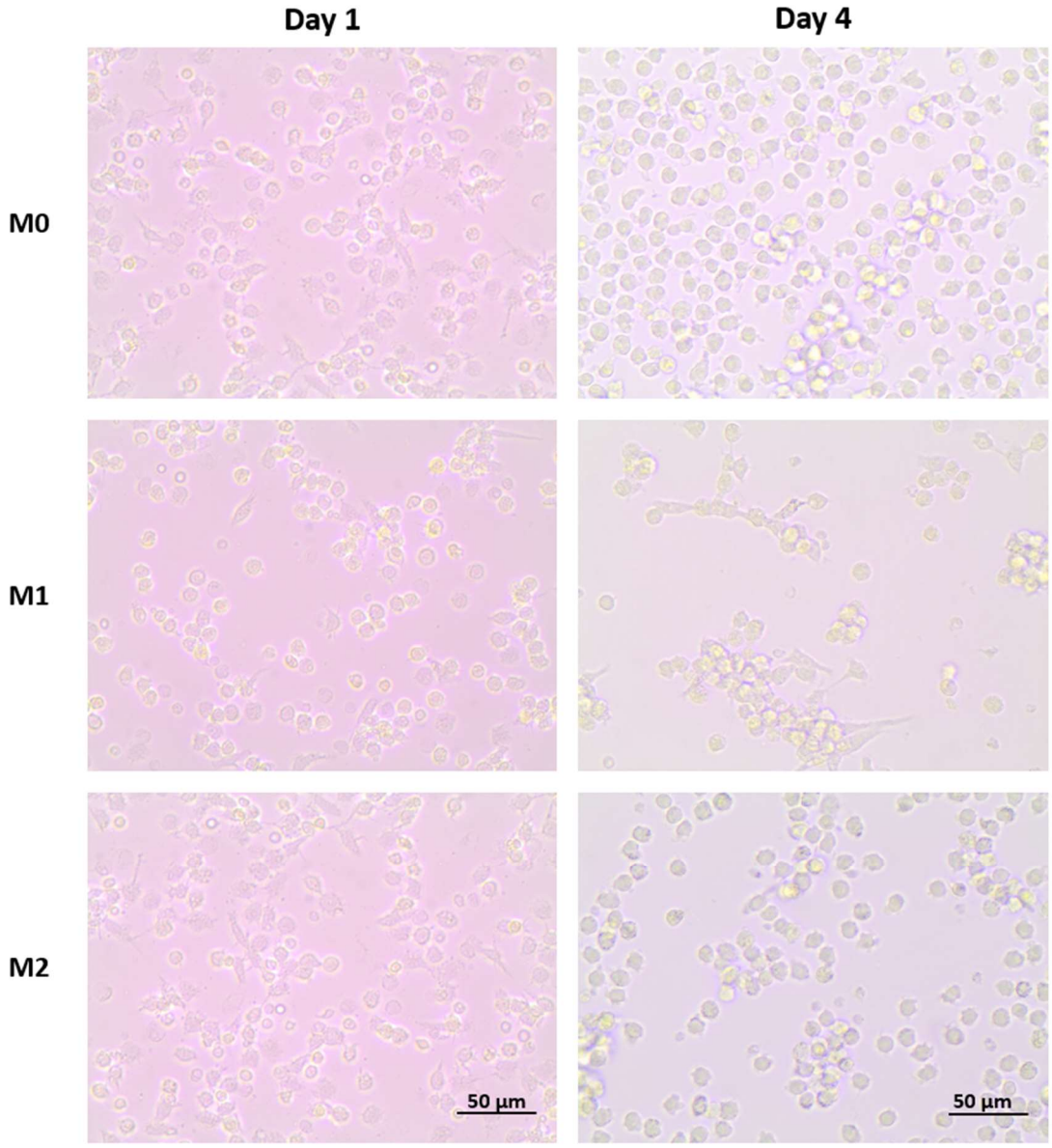

Figure 18: Monocytes differentiation culture under light microscopy (200X). At day 1 they did not present any significant morphological differences. At day 4, M1 cells presented more elongated shape than the M0 and M2 cell types.

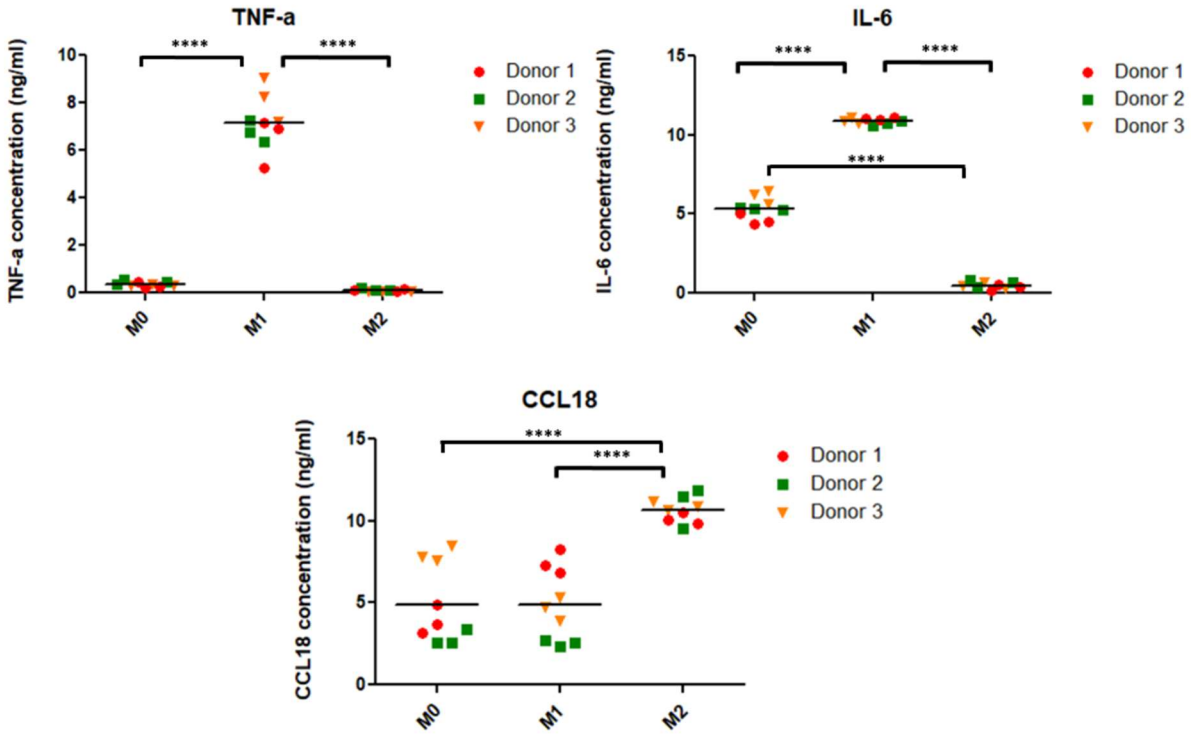

Figure 19: Cytokine concentrations (ng/ml) obtained from ELISA assay after 4 days of culture in monolayers. M1 macrophage phenotype secreted significantly higher levels of pro-inflammatory cytokines IL-6 and TNF-α compared to M0 and M2 phenotypes. CCL18 (anti-inflammatory cytokine) secretion was significantly higher for M2 macrophage phenotype. Data are presented in dot plots and the grand mean (average between N=3 donors) is shown for each sample. A linear mixed model followed by a Bonferroni's *post hoc* test was used for statistical evaluation. ($p \leq 0.05$ (*); $p \leq 0.01$ (**); $p \leq 0.001$ (***); $p \leq 0.0001$ (****)).

Table 4: The average concentration (N = 3 donors) of IL-6, TNF-α and CCL18 produced by M0, M1 and M2 phenotypes.

	TNF-α (ng/ml)		IL-6 (ng/ml)		CCL18 (ng/ml)	
Macrophage phenotype	**Mean**	±	**Mean**	±	**Mean**	±
M0	0.366	0.078	5.347	0.735	4.914	2.702
M1	7.133	0.924	10.884	0.167	4.893	2.456
M2	0.100	0.046	0.487	0.134	10.683	0.481

3.3.2 Effects of implant ion release on human macrophages

After isolation from three different human buffy coats, CD14+ cells were cultured in monolayers in the presence of different titanium implants in transwells in order to evaluate if ions released from implant surface had an effect on human macrophage polarization. Cells were cultured for 4 days. No difference in macrophage morphology in the presence of the three different types of titanium implants, namely SLM NT, SLM PEO and SLM PEO + Ag, was observed after 1 day and 4 days of culture (**Figure 20**). Furthermore, the spherical cell shape in the presence of implants in transwells is similar to the morphology of negative control, composed of undifferentiated macrophages only, without any type of implant.

After 4 days of culture, no significant difference in the release of cytokines was found between the implant groups, for the three different donors investigated (**Figure 21**). All TNF-α, IL-6 and CCL18 concentration values were comparable to the negative control, composed of undifferentiated (M0) macrophages only, without any type of implant. The results are listed in **Table 5**.

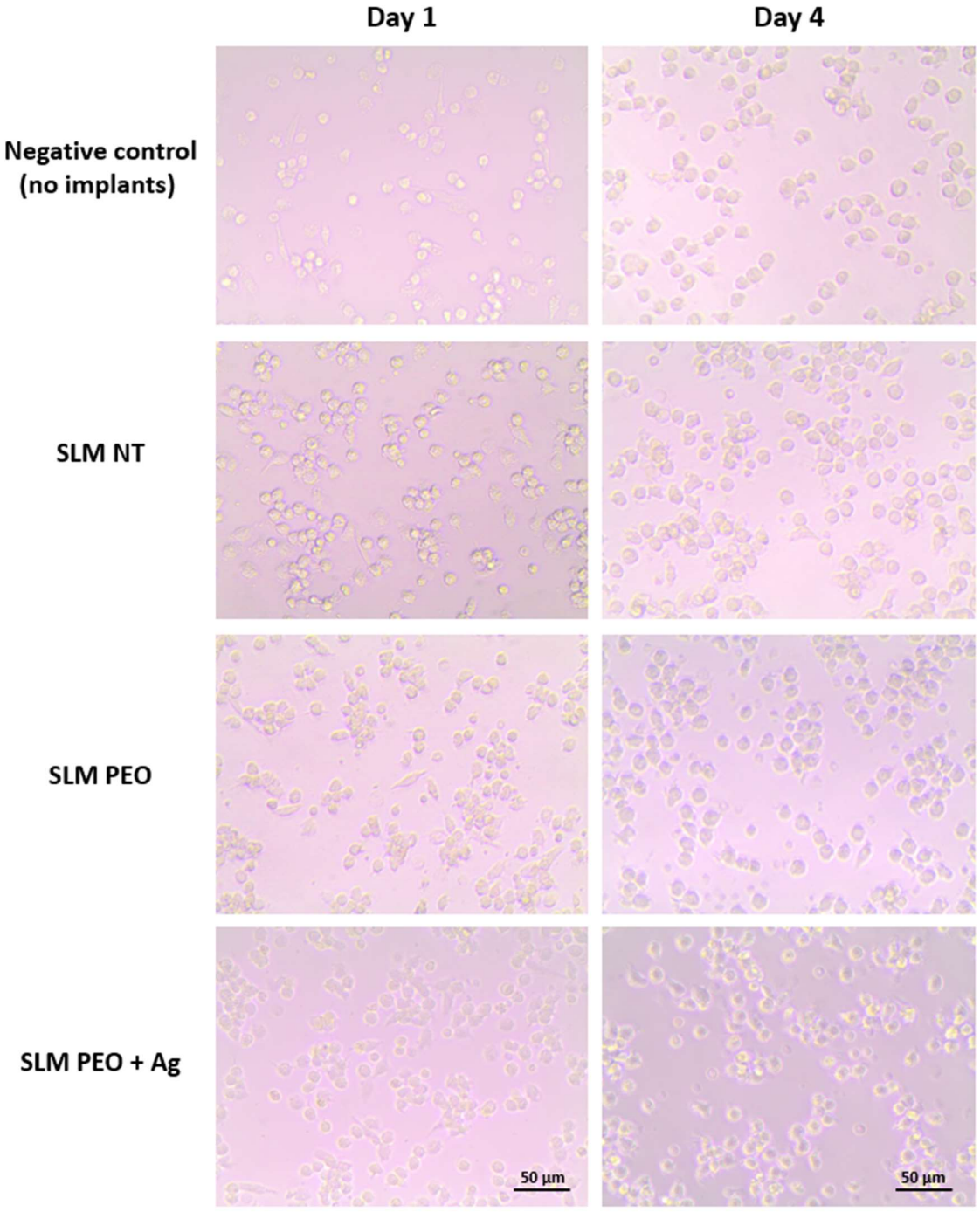

Figure 20: Monocyte culture in monolayers in the presence of SLM in transwells under light microscopy (200X). At day 1 and day 4 there was not any significant morphological differences between the groups investigated.

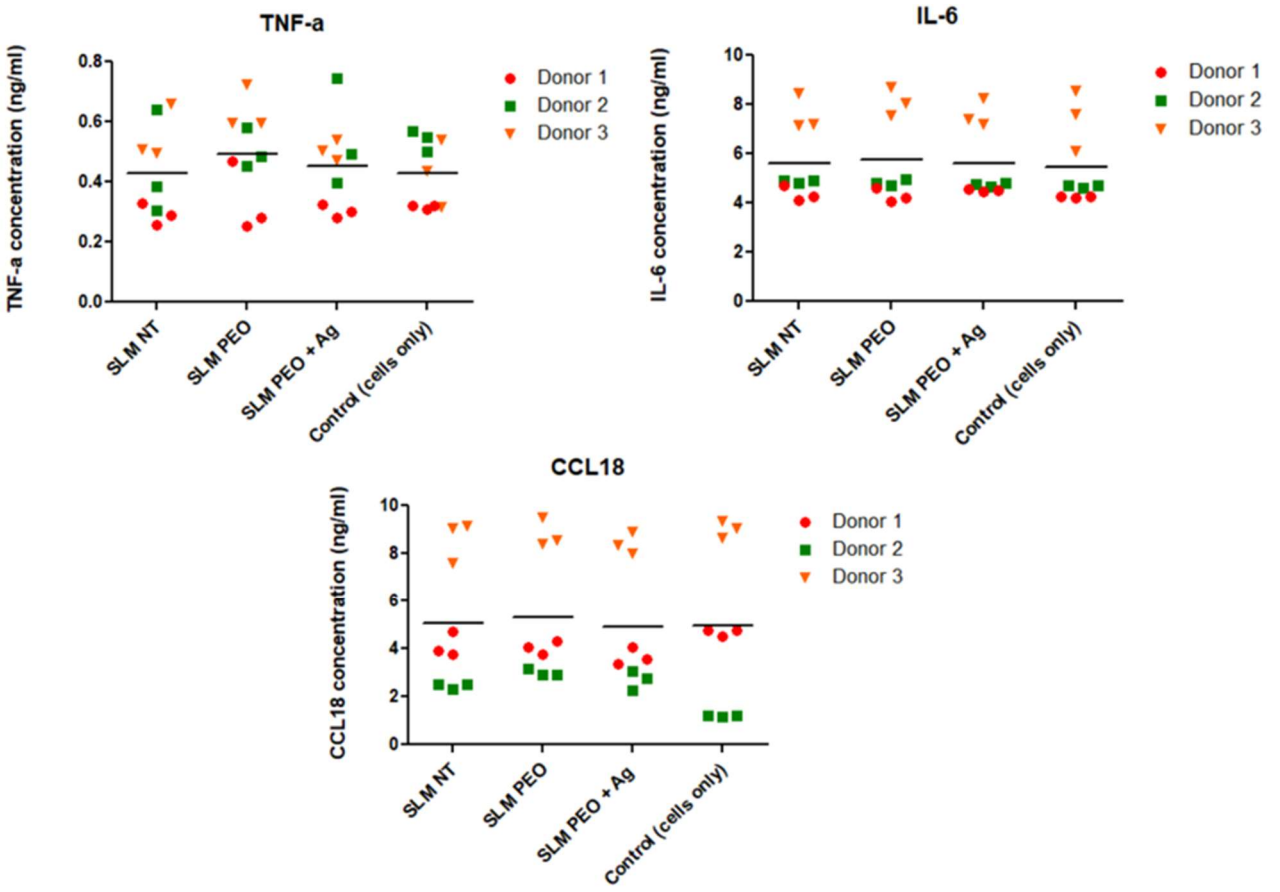

Figure 21: Cytokine concentrations (ng/ml) obtained from ELISA assay after 4 days of culture in monolayers in the presence of SLM implants in transwells. No significant difference was found between the groups. Data are presented in dot plots and the grand mean (average between n=3 donors) is shown for each sample. A negative control was included, composed of CD14+ cells only, without SLM implants in transwells. A linear mixed model followed by a Bonferroni's *post hoc* test was used for statistical evaluation.

Table 5: The average concentration (N = 3 donors) of IL-6, TNF-α and CCL18 produced by CD14+ cells in the presence of SLM implants in transwells.

	TNF-α (ng/ml)		IL-6 (ng/ml)		CCL18 (ng/ml)	
Experimental group	**Mean**	±	**Mean**	±	**Mean**	±
SLM NT	0.431	0.152	5.612	1.559	5.058	2.804
SLM PEO	0.493	0.154	5.747	1.815	5.294	2.712
SLM PEO + Ag	0.451	0.146	5.623	1.526	4.931	2.677
Control (cells only)	0.429	0.113	5.446	1.617	4.956	3.408

3.3.3 Culture of human macrophage on Ti-6Al-4V surfaces

Human CD14+ cells were isolated from a buffy coat and cultured on SLM NT, SLM PEO and SLM PEO + Ag implants. Cell morphology, viability, protein secretion and gene expression were analysed after of culture in order to investigate macrophage polarization.

3.3.3.1 Human macrophage morphology

Macrophage adhesion and morphology was evaluated after 4 days of culture on the implants by SEM. Images were taken at different magnifications as explained in methods section. Here, implant images at four different magnifications are shown, namely 100X 200x, 500x and 1000x. In the pictures, cells are visible because of their darker appearance compared to titanium. On the SLM NT implants (**Figure 22**), cells attached homogeneously to the surface, especially in surface smoother parts. Cell shape was mostly rounded. On the other hand, macrophages attached to SLM PEO surfaces showed a more elongated shape and such cells were found mostly in surface pores (**Figure 23**). Finally, a considerable amount of cells was found on SLM PEO + Ag surfaces (**Figure 24**). These cells had rounded shape and smaller dimensions compared to cells attached on the other two types of implants. SEM images were taken for five different donors.

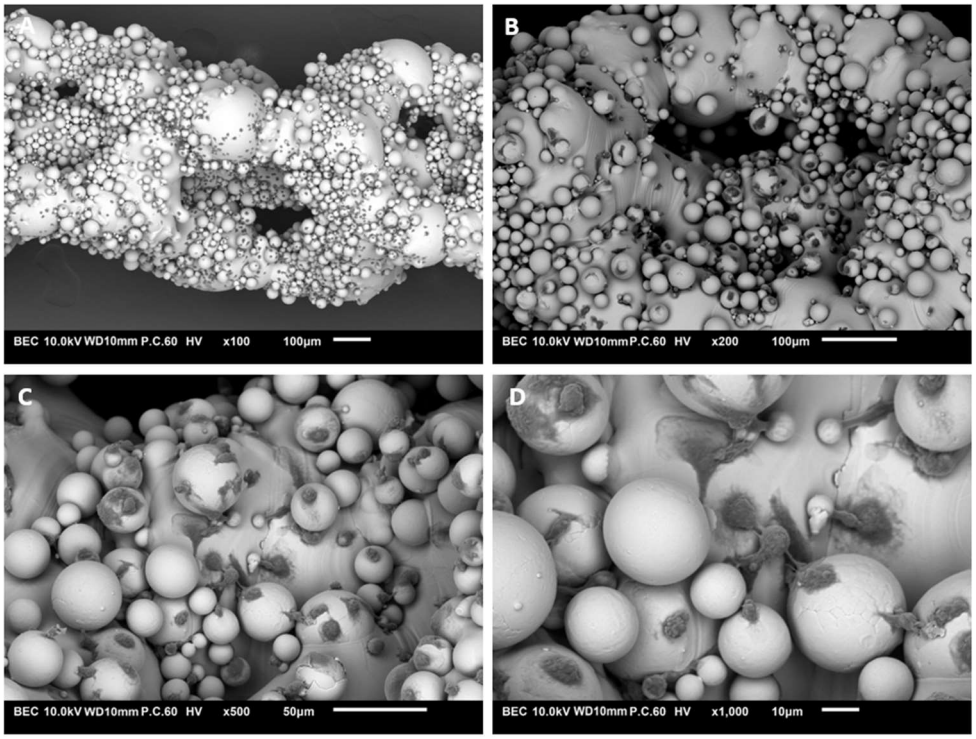

Figure 22: Human macrophage morphology on SLM NT implants after 4 days of culture (100X, 200X, 500X, 1000X). Cells uniformly attached to implant surface. The morphology was mostly rounded.

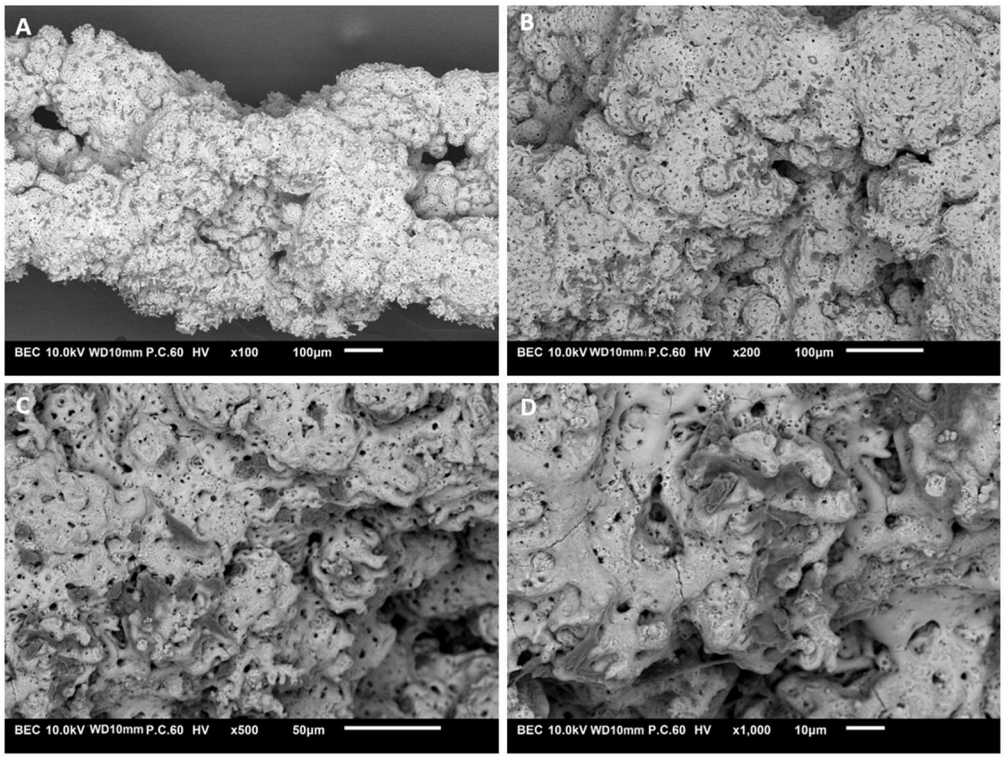

Figure 23: Human macrophage morphology on SLM PEO implants after 4 days of culture (100X, 200X, 500X, 1000X). Cells uniformly attached to implant surface. The morphology was mostly elongated.

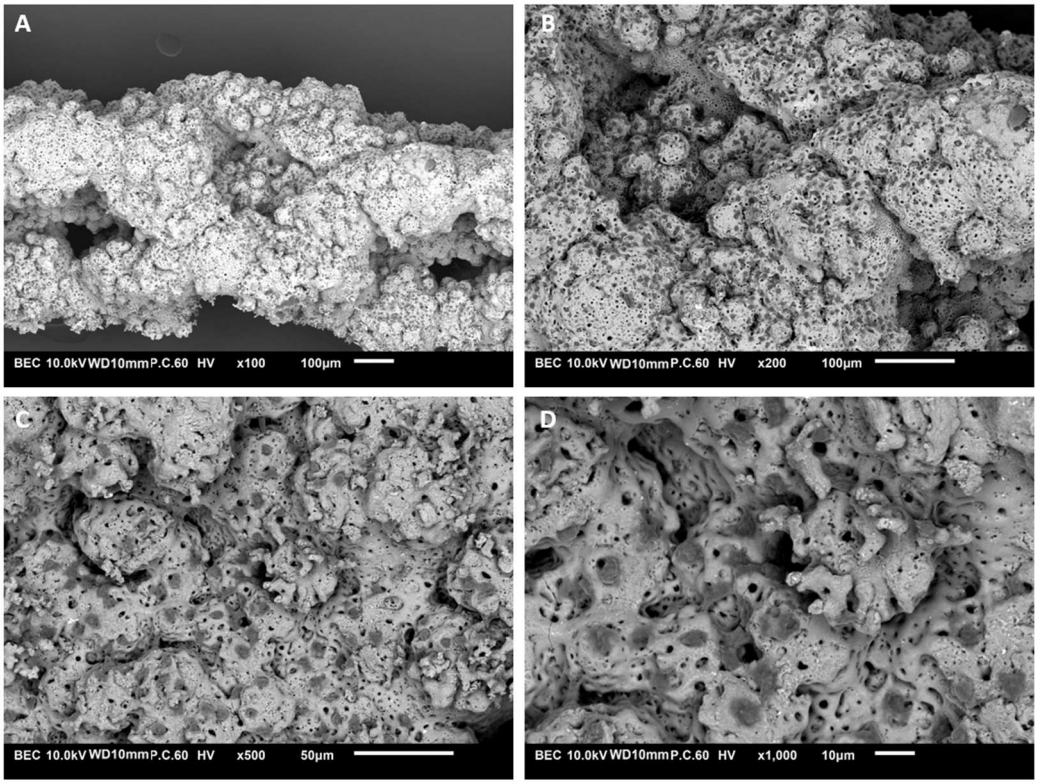

Figure 24: Human macrophage morphology on SLM PEO + Ag implants after 4 days of culture (100X, 200X, 500X, 1000X). Cells uniformly attached to implant surface. The morphology was mostly rounded.

3.3.3.2 Human macrophage viability

In order to evaluate SLM implant cytotoxicity for cultured macrophages, cell viability was investigated with a live/dead assay. Two different dyes were used to stain live and dead cells, namely calcein AM, green, and ethidium homodimer, red. Neither SLM NT nor SLM PEO were cytotoxic for human macrophages after 4 days of culture (**Figure 25.A,B**). In addition, these images show that cell attachment was uniform along the implant and few dead cells were found compared to live ones. However, the number of cells attached to SLM NT surfaces was higher compared to SLM PEO ones. On the other hand, SLM PEO + Ag surface had cytotoxic effects on human macrophages (**Figure 25.C**), which died after 4 days of culture. However, the cells were still uniformly attached to the surface.

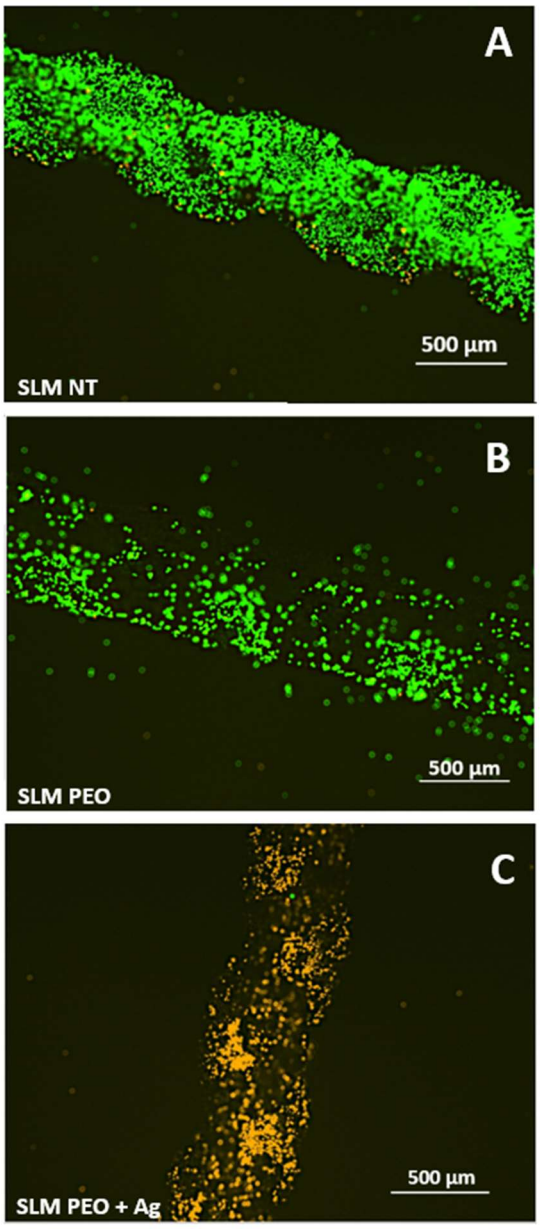

Figure 25: Live/dead staining of human macrophages on SLM NT (A), SLM PEO (B) and SLM PEO + Ag (C) implants after 4 days of culture. Green colour indicates live cells and orange colour the dead ones.

3.3.3.3 Analysis of pro- and anti-inflammatory cytokine secretion

After 4 days of culture of macrophages on the SLM implants, cell supernatant was collected and an ELISA assay to assess IL-6 (pro-inflammatory cytokine) and CCL18 (anti-inflammatory) concentration (ng/ml) was performed. Regarding IL-6 secretion (**Figure 26**), donor 1 macrophages secreted less than 0.2 ng/ml, for all the experimental groups. On the other hand, IL-6 secretion for all the other donors (donor 2, 3, 4, 5) presented a similar trend, with up-regulation of IL-6 secretion from cells cultured on SLM NT implants compared to macrophages cultured on SLM PEO implants. For all donors, IL-6 secretion from cells cultured on SLM PEO + Ag implants was undetectable. CCL18 concentration was similar for cells adhered to SLM NT and SLM PEO groups for donor 1 and 2. Donor 3 and 5 macrophages secreted higher amounts of CCL18 when cultured to SLM PEO compared to SLM NT group, while for donor 4 the anti-inflammatory cytokine was secreted only by cells cultured on non PEO-treated titanium implants. CCL18 was not detectable in supernatant of macrophages cultured on surfaces containing Ag NPs (**Figure 26**).

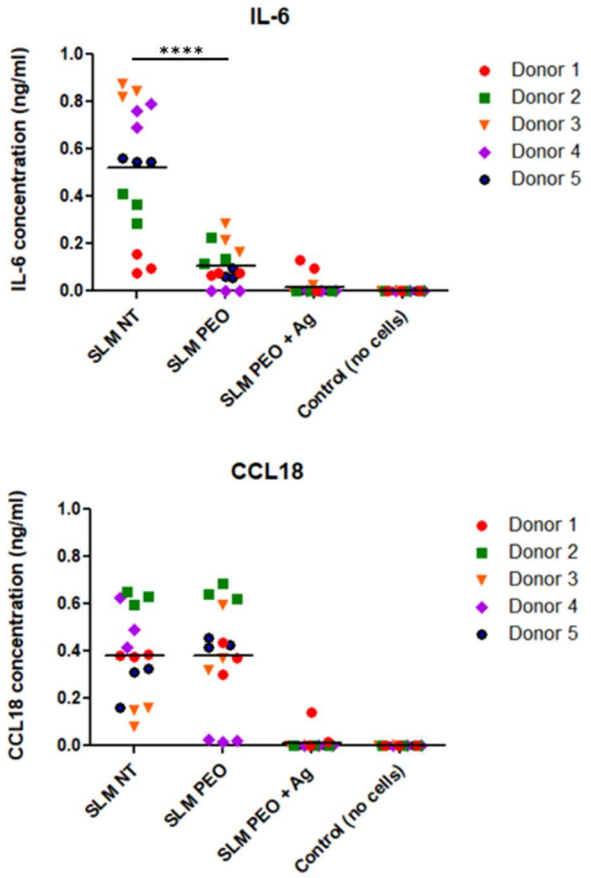

Figure 26: IL-6 and CCL18 concentration (ng/ml) in macrophage supernatant after 4 days of culture as revealed by ELISA assay. SLM NT implants up regulated macrophage IL-6 secretion while no significant difference was found between SLM NT and SLM groups regarding CCL18 secretion. Cells cultured on SLM PEO + Ag implants did not secrete IL-6 and CCL18 after 4 days of culture. Data are presented in dot plots and the grand mean (average between N=3 donors) is shown for each sample. The negative control was composed of SLM implants, without macrophages cultured on them. A linear mixed model followed by a Bonferroni's *post hoc* test was used for statistical evaluation. A linear mixed model followed by a Bonferroni's *post hoc* test was used for statistical evaluation. ($p \leq 0.05$ (*); $p \leq 0.01$ (**); $p \leq 0.001$ (***); $p \leq 0.0001$ (****)).

However, these results show only the total concentration of cytokines in culture medium, without taking into account the number of the cells adhered. In order to do this, after 4 days of culture, adhered cells were harvested and DNA quantification assay was performed for three donors out of five, namely donor 3, 4 and 5 (**Figure 27.A**). DNA content on SLM NT implants was significantly higher compared to SLM PEO and SLM PEO + Ag group, for all three donors. No significant difference was observed in DNA content between the SLM PEO and SLM PEO + Ag group. The DNA quantification results were used to normalize the ELISA assay values. As a result of such normalization (**Figure 27.B,C**), it was found that SLM PEO treated surfaces down-regulated adherent macrophages secretion of the pro-inflammatory cytokine IL-6 and up-regulated the anti-inflammatory cytokine CCL18 secretion compared to cells cultured on SLM NT surfaces. As shown before, cytokines were not detectable in culture medium of cells adhered on SLM PEO + Ag implants. All the values are listed in **Table 6**.

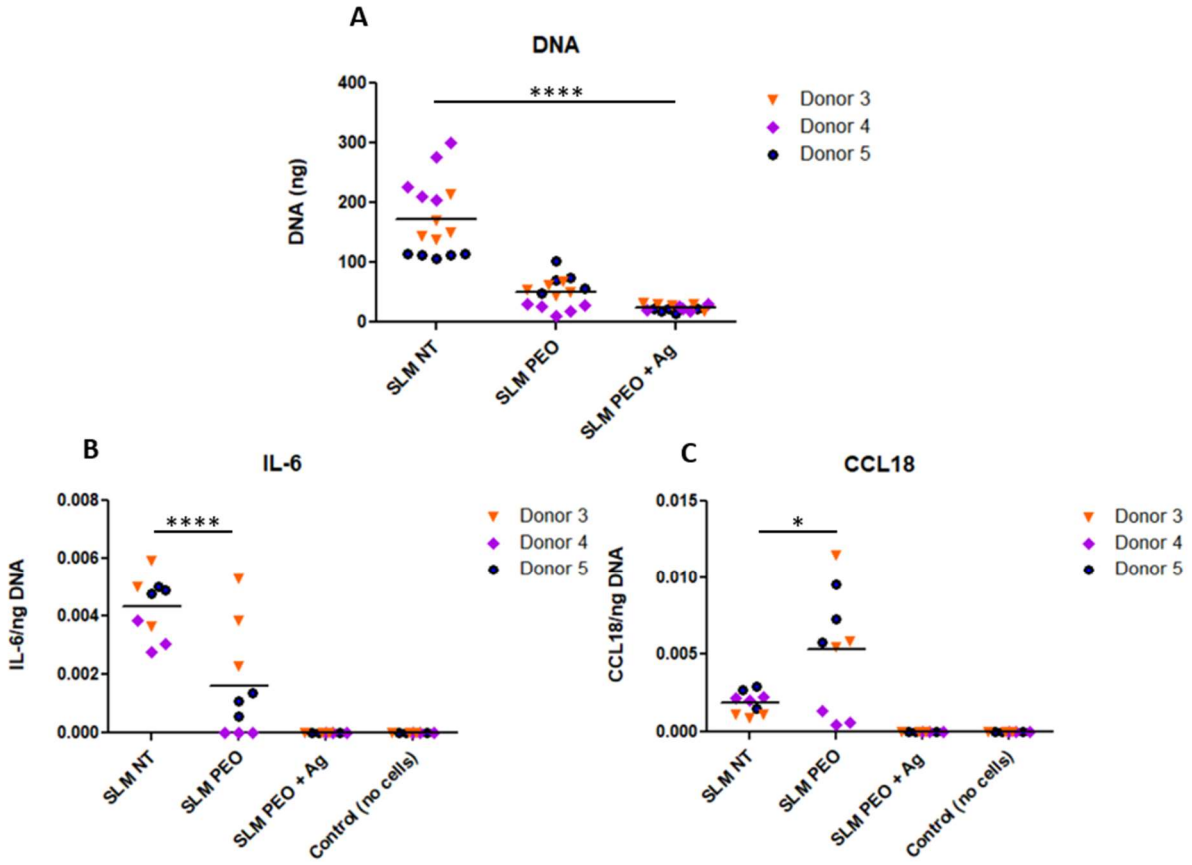

Figure 27: (A) DNA quantification of human macrophages cultured on SLM implants. DNA was significantly higher for cells cultured on SLM NT compared to the other two groups. (B,C) Secreted cytokines values (IL-6, CCL18) (ng/ml) obtained from ELISA assay corrected for DNA content (ng) after 4 days of culture on the SLM implants. SLM NT surfaces up-regulated macrophage IL-6 secretion compared to SLM PEO, while SLM PEO surfaces up-regulated macrophage CCL18 secretion. Data are presented in dot plots and the grand mean (average between N=3 donors) is shown for each sample. The negative control was composed of SLM implants, without macrophages cultured on them. A linear mixed model followed by a Bonferroni's *post hoc* test was used for statistical evaluation. A linear mixed model followed by a Bonferroni's *post hoc* test was used for statistical evaluation. ($p \leq 0.05$ (*); $p \leq 0.01$ (**); $p \leq 0.001$ (***); $p \leq 0.0001$ (****)).

Table 6: The average concentration (N = 3 donors) of IL-6, and CCL18 produced by macrophages when cultured on SLM NT, SLM PEO and SLM PEO + Ag implants.

	IL-6 (ng/ml)		CCL18 (ng/ml)	
Experimental group	**Mean**	±	**Mean**	±
SLM NT	0.0043	0.0010	0.0019	0.0007
SLM PEO	0.0016	0.0019	0.0053	0.0039
SLM PEO + Ag	0.0000	0.0000	0.0000	0.0000
Control (no cells)	0.0000	0.0000	0.0000	0.0000

3.3.3.4 Gene expression analysis

After 4 days of macrophage culture on titanium surfaces, cells were treated with TRIzol reagent in order to disrupt adhered cells and isolate RNA. cDNA was synthesized and it was used as template for gene expression analysis by qPCR. Both pro- and anti-inflammatory factors were investigated (see **Table 2**). Due to undetectable gene expression from cells cultured on SLM PEO + Ag, this experimental group was excluded from the analysis and only the results for SLM NT and SLM PEO groups are shown (**Figure 28**). All the values were normalized to GAPDH expression, which was chosen as the best housekeeper. The difference of the mean between the two groups was considered statistically significant for p values lower than 0.05. According to pro-inflammatory cytokines, IL1-β, IL-6 and TNF-α expression was investigated. PEO-treated surfaces significantly down-regulated the expression of these cytokines for all five donors. In general, IL-6 expression was low for cells cultured on SLM NT group and undetectable for all the cells cultured on SLM PEO group. As anti-inflammatory cytokines, the expression of CCL18, IL1-RA, IL-10 was investigated. No difference was found between the two groups regarding CCL18 and IL-10 secretion, while IL1-RA expression was significantly higher for cells adhered on SLM NT group. TGF-β was expressed by both groups, with no significant difference. Interestingly, M2 phenotype surface marker expression, namely CD163 and CD206, presented an opposite trend. CD163, surface marker of macrophage subtype M2c, was significantly up regulated by PEO-treated surfaces, while cells cultured on non-treated implants expressed significantly higher values of CD206, surface marker of macrophage subtype M2a. VEGF expression was not detectable for any experimental group and donor (data not shown). A summary of gene expression analysis results is presented in **Table 7**.

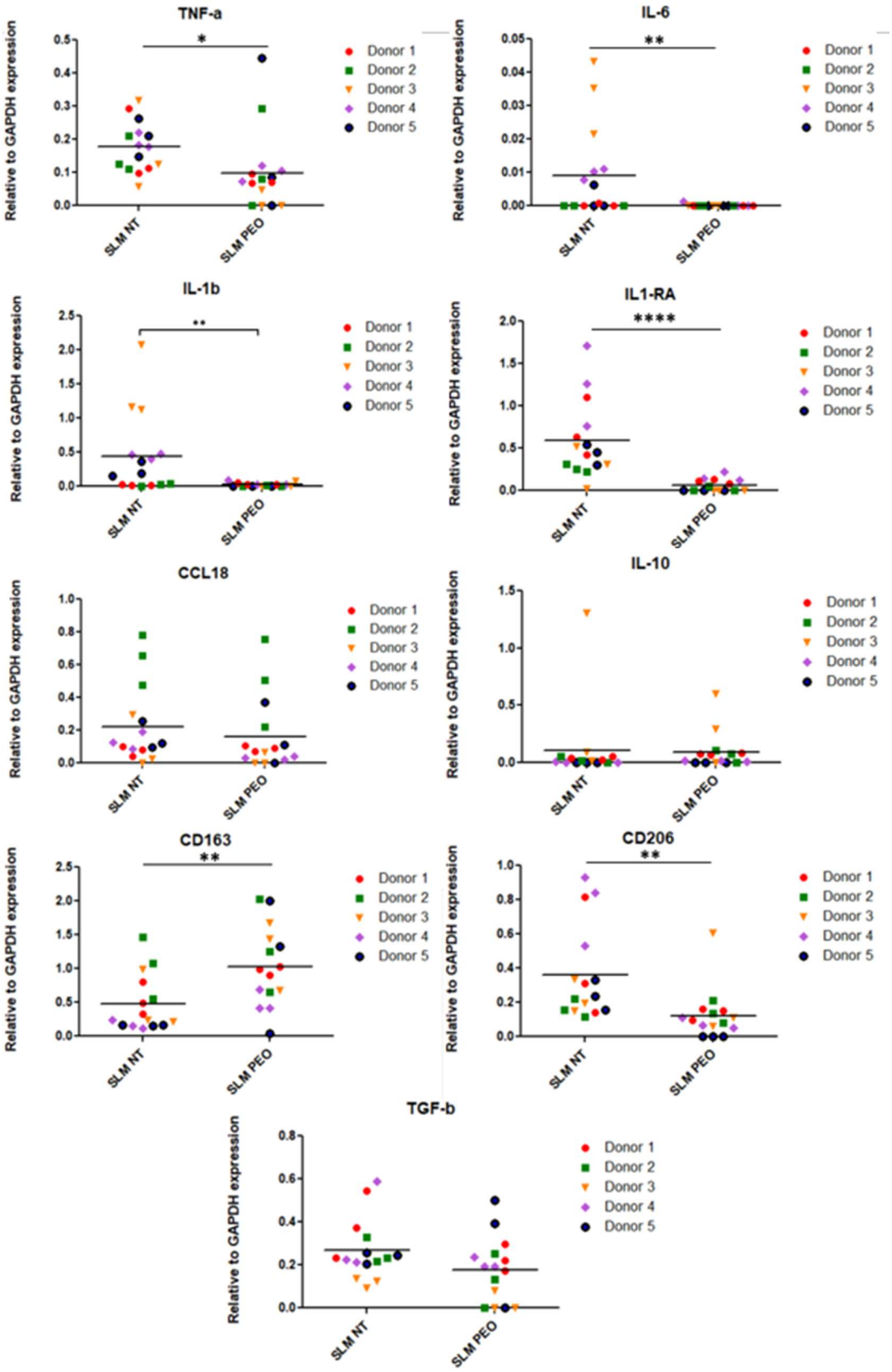

Figure 28: Expressed genes by human macrophages cultured on SLM NT and SLM PEO implants after 4 days of culture. Data are presented in dot plots and the grand mean (average between n=3 donors) is shown for each sample. A linear mixed model followed by a Bonferroni's *post hoc* test was used for statistical evaluation. A linear mixed model followed by a Bonferroni's *post hoc* test was used for statistical evaluation. ($p \leq 0.05$ (*); $p \leq 0.01$ (**); $p \leq 0.001$ (***); $p \leq 0.0001$ (****)).

Table 7: Gene expression analysis results for human macrophages cultured on SLM NT and SLM PEO surfaces. (↑ = up regulated; ↓ down regulated; = = no significant difference between the groups; - = not expressed).

Genes		SLM NT	SLM PEO
Pro-inflammatory cytokines	IL-1β	↑	↓
	IL-6	↑	↓
	TNF-α	↑	↓
Anti-inflammatory cytokines	IL-1RA	↑	↓
	IL-10	=	=
	CCL18	=	=
Anti-inflammatory surface markers	CD163	↓	↑
	CD206	↑	↓
Growth factors	VEGF	-	-
	TGF-β	=	=

3.4 *In vitro* evaluation of hMSCs response to SLM implants

3.4.1 hMSC morphology

hMSC morphology was evaluated after 4 days of culture on the implants by SEM. Images were taken at different magnifications as explained in method section. Here, implant images at two different magnifications are shown, namely 100X and 500x. In the pictures, cells are visible because of their darker appearance compared to titanium. Cells attached homogeneously to all the surfaces investigated, with no substantial differences in morphology and adhesion (**Figure 29**).

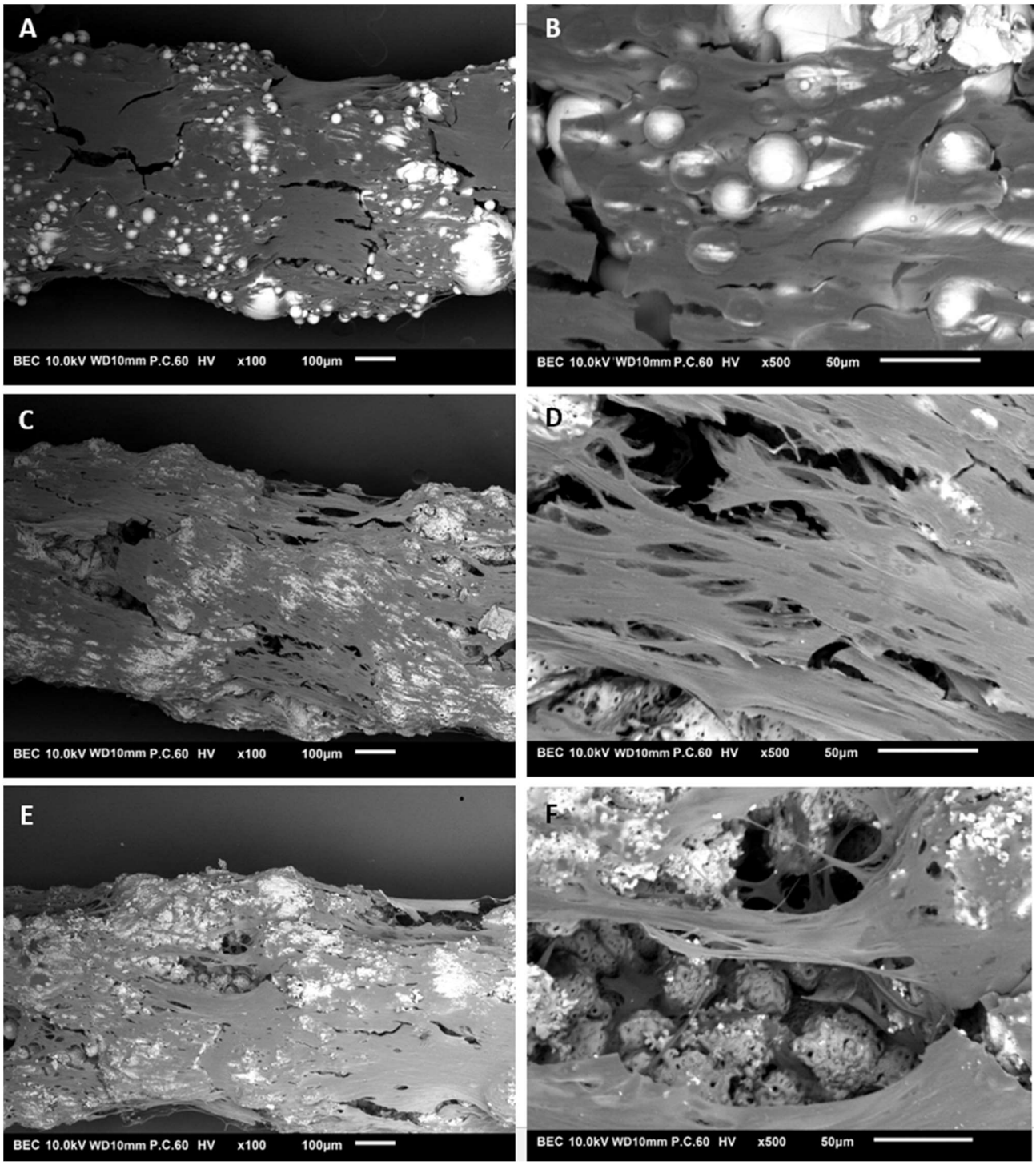

Figure 29: Human MSC morphology on SLM implants after 4 days of culture. Cells attached uniformly with no substantial differences in morphology on SLM NT (a,b), SLM PEO (c,d) and SLM PEO + Ag (e,f).

3.4.2 hMSC viability

In order to evaluate SLM implant cytotoxicity for cultured hMSCs, cell viability was investigated with a live/dead assay. Two different dyes were used to stain live and dead cells, namely calcein AM, green, and ethidium homodimer, red. SLM NT, SLM PEO and SLM PEO + Ag were all not cytotoxic for hMSCs after 4 days of culture (**Figure 30**). Cell attachment was uniform along the implant and few dead cells were found compared to live ones on the surface.

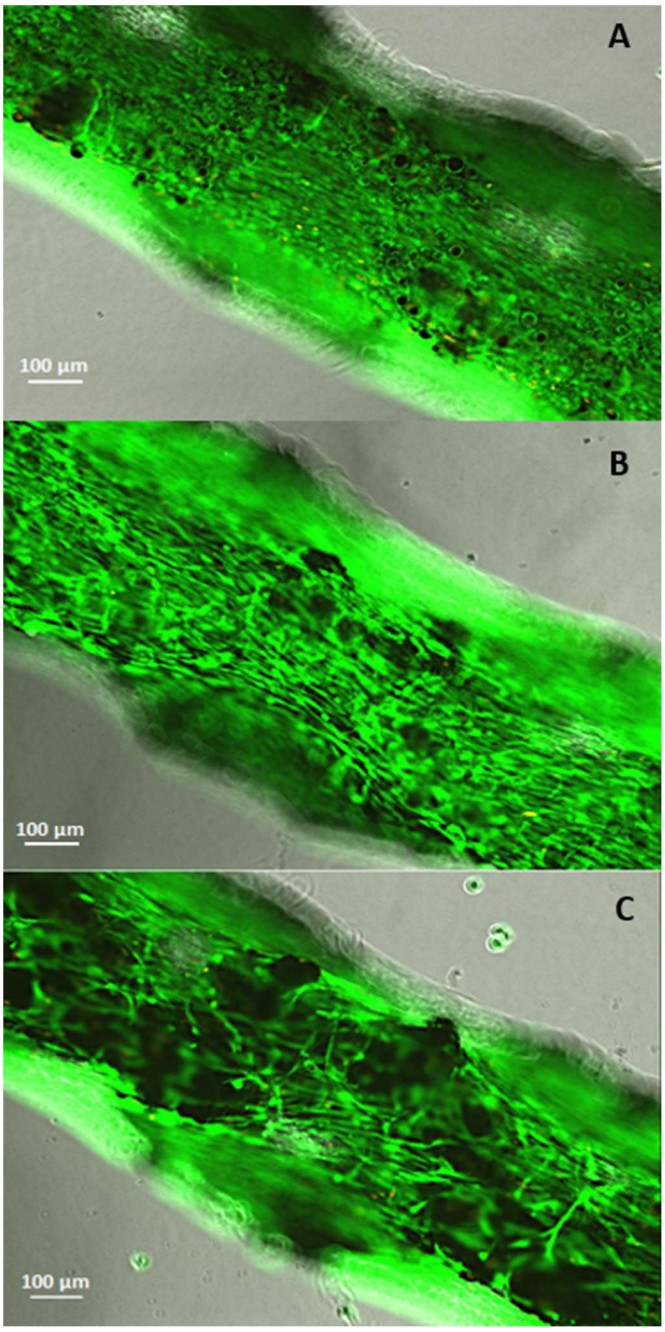

Figure 30: Live/dead staining of hMSCs on SLM NT (A), SLM PEO (B) and SLM PEO + Ag (C) implants after 4 days of culture. Green colour indicates live cells and orange colour the dead ones.

3.5 *In vitro* evaluation of macrophage/MSC interaction

The human macrophages were cultured on SLM NT, SLM PEO and SLM PEO + Ag implants. After 2 days of culture, the macrophage-conditioned medium (MCM) was collected. A DNA assay was performed in order to correct the MCM for the number of cells that conditioned the medium. The DNA results per well were summed and the CM percentage was calculated accordingly, as explained in section 2.6.1 Macrophage-condition medium (MCM) preparation(**Table 8**).

Table 8: Preparation of MCM. DNA content was measured for each well, containing n=3 SLM implants. DNA values (ng) per condition were summed together. The total DNA values for all the three conditions (SLM NT = 1193.22 ng; SLM PEO = 686.19 ng; SLM PEO + Ag = 1060 ng) were averaged and the resulting average was considered as 50%. The MCM percentage for each condition was calculated accordingly.

	DNA (ng)	% MCM
SLM NT	1193.22	39.12
SLM PEO	686.19	64.99
SLM PEO + Ag	1060.237	45.90

A migration assay of MSCs using MCM was performed and the number of migrated cells in response to different CMs was evaluated (**Figure 31**). The number of migrated cells was higher in the presence of MCM obtained from macrophages cultured on SLM NT (4376.87 ± 269.10) and SLM PEO group (4189.66 ± 758.60), compared to SLM PEO + Ag group (3036.12 ± 1052.92). Interestingly, these values obtained for migrated cells in MCM were higher than the migrated cells in medium containing 1% (2046.71 ± 165.00) and 10% (2760.59 ± 151.02) FBS only, without factors released from macrophages.

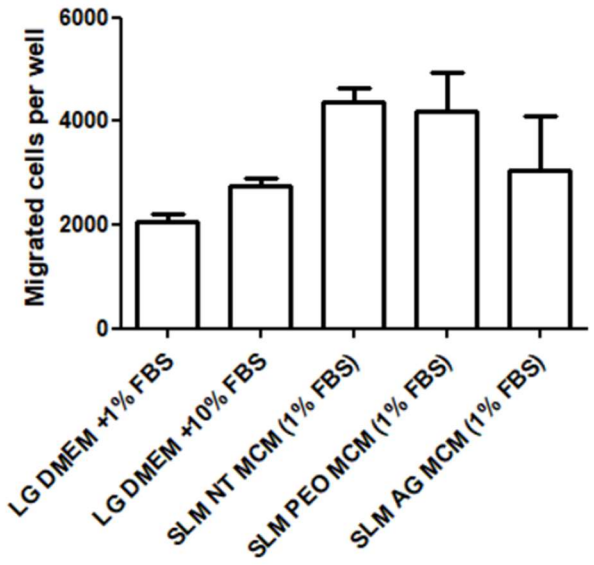

Figure 31: Number of migrated cells obtained from a migration assay of MSCs in macrophage-CM. The number of migrated cells in the presence of factors released by macrophages (SLM NT, SLM PEO and SLM PEO + Ag MCM) was higher compared to migrated cells using CM containing FBS only (1% and 10% FBS). No significant difference was found between the groups. A linear mixed model followed by a Bonferroni's *post hoc* test was used for statistical evaluation. A linear mixed model followed by a Bonferroni's *post hoc* test was used for statistical evaluation.

4. Discussion

The aim of this thesis research was to evaluate the *in vitro* human macrophage response to modified 3D printed bone implants. A surface modification by PEO was applied to 3D printed Ti-6Al-4V implants. As a result, two different surfaces were synthesized: a PEO treated surface and a PEO treated surface with an additional incorporation of Ag NPs. The presence of Ag NPs was previously shown to increase antimicrobial activity of such implants [9]. However, IAI resulting from initial microbial adhesion is not the only cause of bone implant failure. For example, aseptic loosening and poor bone ingrowth are also responsible for unsuccessful implant integration in the human body [3]. Once implanted, biomaterial surface influences host tissue response, including early immune system response and subsequent osteogenesis. Thus, an ideal bone implant should be able to avoid the risk of IAI while promoting new bone formation through modulation of initial inflammatory response. Such desirable properties are called osteoimmunomodulatory properties, as defined recently by Chen *et al.* [12,21]. However, while bone-forming cell response to bone titanium implants has been extensively investigated in recent literature, knowledge about the response of macrophages, key players in osteoimmunomodulation, is still limited. In this study, the effects of titanium surface ion release and effects of surface itself upon contact with human macrophages on their polarization and on MSCs migration were investigated using cells from different human donors, which gives an additional clinical relevance to this research.

4.1 Effects of PEO treatment

Implant PEO treatment was performed by applying a constant current density to the titanium implants while immersed in an electrolyte containing calcium acetate and calcium glycerophosphate with or without silver nanoparticles. During PEO process, the steep voltage increase observed during the first *ca* 10 seconds represented the generation of an amorphous titanium oxide layer [37]. Once dielectric breakdown occurred, porous structures and complex compounds containing electrolyte components were formed. In the V transient curve, this process corresponds to the slowing down in voltage increase. No differences were observed according to the voltage curves between the two types of surfaces generated, showing that the presence of Ag NPs in the electrolyte did not affect the oxide layer growth kinetics. The titanium implants synthesized with PEO treatment presented a porous TiO_2 layer with interconnected pores and micro-cracks. Such topographical features resulted in an increased surface roughness, which may influence host cell adhesion as well as cell/biomaterial interaction [38]. During PEO process, electrolyte components such as Ca, P as well as Ag NPs were successfully incorporated on the surface. In addition, previous studies showed the presence of specific phases by X-ray diffraction (XRD) analysis on the SLM PEO surface revealing the presence of Ti6Al4V, anatase, rutile, $Ca_3(PO_4)_2$, hydroxyapatite, perovskite and ($CaTiO_3$) phases, and the release of Ag

ions from the surface [9]. The effects of such PEO treated surfaces on human macrophage polarization are discussed in the next sections.

4.1.1 Human macrophage adhesion and morphology

PEO treatment altered implant surface in terms of topography and chemical composition. With regard to cell adhesion, DNA assay quantification results showed that more cells were attached to the SLM NT surfaces after 4 days of culture compared to SLM PEO and SLM PEO + Ag surfaces. This may be due to the increased roughness of PEO-treated surfaces. Even though SLM NT implants presented rough surface due to residual metal powder, cells were mostly found on the smoother parts of these surfaces. Higher cell attachment to smooth surfaces compared to rough ones was also reported by Hotchkiss *et al.* [39]. SEM analysis revealed differences in cell morphology between the groups. The more elongated shape observed on the SLM PEO surfaces may be due to implant surface topography, which leads to cell adaptation to surface patterns and migration. In addition to this, Lee et al. demonstrated that macrophage morphology reflects their activation state. Activated cells are more stretched, as a consequence of migration, whereas inactivated cells are more rounded [40].

Cell viability was assessed performing a live/dead assay of macrophages cultured over a period of 4 days on the SLM implants. Macrophages were found alive and uniformly distributed on SLM NT and SLM PEO surfaces. On the other hand, a considerable amount of cells was observed on SLM PEO + Ag implants. However, the cells presented smaller dimension compared to cells cultured on the two other SLM surfaces, and cell DNA content was significantly lower. Cell shrinkage is a typical feature of cells undergoing apoptosis [41], and results from live/dead assay as well as protein secretion and gene expression analysis performed in this study may be in line with this hypothesis. However, further investigation is needed to understand the death mechanism of macrophages cultured on SLM PEO + Ag surfaces.

4.1.2 Human macrophage polarization in response to SLM Ti-6Al-4V implants

The effects of SLM surfaces on human macrophage polarization were investigated after 4 days of culture. As explained previously, this immune cell type plays a crucial role in osteoimmunomodulation after biomaterial implantation; its early response influences both inflammatory phases and tissue repair and new bone formation through secretion of a wide spectrum of pro-, anti-inflammatory and tissue repair-related factors [12].

In this study, some of commonly pro- and anti-inflammatory macrophage secreted factors were investigated by ELISA assay and gene expression analysis. As discussed previously, surfaces bearing Ag NPs were found to be cytotoxic for human macrophages, which secreted and expressed undetectable levels of the factors analysed. Thus, in this section, only the difference between SLM NT and SLM PEO implants is discussed.

On protein level, assessed by ELISA assay, not treated (SLM NT) surface significantly up regulated IL-6 secretion while SLM PEO surface significantly up regulated CCL18 secretion, even though detected DNA values on PEO-treated surfaces were lower. IL-6 is mostly secreted by M1 macrophage phenotype [17], and it is known that a prolonged secretion of pro-inflammatory cytokines can have a negative impact on tissue healing phase, leading to fibrous encapsulation of the implant [12]. Some studies also reported that it may inhibit maturation and differentiation of osteoblasts [42]. On the other hand, during wound healing, IL-6 has been shown to modulate granulation tissue formation and to be involved in bone resorption and formation [43,44]. CCL18, also known as macrophage activation associated CC-chemokine is a member of the CC-chemokine family and it is produced by cells of myeloid origin. Such cytokine has been shown to be a maturation factor for monocytes, promoting the differentiation towards a M2 phenotype [79]. Furthermore, such factor plays important roles in tissue remodelling phase [45].

According to gene expression analysis, TNF-α, IL1-β and IL-6 (pro-inflammatory cytokines), IL-1RA, IL-10, and CCL18 (anti-inflammatory cytokines), TGF-β and VEGF (tissue repair-related growth factors), CD163 and CD206 (M2 macrophage surface markers) were investigated. Pro-inflammatory cytokine expression was significantly higher for cells cultured on SLM NT group compared to SLM PEO one for all donors. In line with ELISA results, SLM PEO significantly down-regulated the expression of pro-inflammatory cytokines (IL-1β, IL-6 and TNF-α). This can be attributed to the altered topography and chemical composition of the PEO-surface [46,47]. Furthermore, the presence of HA may enhance implant biocompatibility and recent studies showed that such presence down-regulated the macrophage pro-inflammatory gene expression [48,49]. TNF-α and IL-1β are considered indicators of the inflammatory response acute phase. Such factors recruit other inflammatory cells to the implant site and some studies reported that they can induce osteoblast apoptosis as well as inhibit osteoblast differentiation, having detrimental effects on healing, both *in vitro* and *in vivo* [50,51,52]. On the other hand, TNF-α and IL-1β have been also shown to be implicated in angiogenesis, regulation of osteoblast and fibroblast proliferation during wound healing [53–55,56].

With regard to anti-inflammatory cytokines, only IL-1RA expression difference was found to be significant; IL1-RA expression was up regulated by cells cultured on SLM NT surfaces compared to SLM PEO ones, while ,with regard to CCL18 expression, no difference was found between the experimental groups for all donors. IL-10 was low or not expressed for most of the donors. IL1-RA and IL-10 are both anti-inflammatory cytokines, whose main function during the early stage of inflammation after biomaterial implantation is to inhibit pro-inflammatory cytokine production [57].

Interestingly, according to surface marker expression, an opposite trend was found between the two groups: CD206 expression was up regulated by SLM NT surfaces while CD163 expression was up regulated by cells on SLM PEO implants. These markers are both present on the surface of M2 macrophage phenotype. In particular, CD206 is a marker for M2a macrophage subtype while CD163 is a marker for M2c one. Opposite opinions are present in literature regarding the functions attributed to M2a and M2c macrophage subtypes.

M2a macrophage subtype has been reported to have an additional role in wound healing, tissue remodelling and repair [58,59], and M2c has been reported to be mainly anti-inflammatory, down-regulating the production of pro-inflammatory cytokines [16]. On the other hand, as Sridharan et al. reported, M2a may also have anti-inflammatory function and M2c macrophage subtype may be involved in matrix deposition, tissue remodelling and pro-healing processes [57].

M2 macrophage phenotype secretes also some factors involved in wound healing and tissue remodelling such as TGF-β1 and VEGF. In particular, TGF-β1, key signalling molecule of the TGF-β superfamily, is involved in the stimulation of osteogenesis and angiogenesis [56]. In the present study, the expression of VEGF was not detectable for all experimental groups and donors. Conversely, all groups and donors expressed TGF-β1, with no significant difference in expression between SLM NT and SLM PEO groups. TGF-β1 and IL-1β interplay in the context of macrophage/implant interaction. These two factors are considered antagonist factors since their presence may be responsible for the transition from a M1 phenotype, during which the secretion of IL-1β is up-regulated, to the wound healing phase, during which the macrophage secreted factor TGF-β1 plays a crucial role [60], enhancing proliferation and differentiation of osteoblast precursors and stimulating angiogenesis [61]. Interestingly, in the culture model investigated, after 4 days of culture, macrophages on SLM PEO surfaces did not express IL-1β, while TGF-β1 was expressed by the same cells for most of the donors.

Taken together, the results suggest that PEO-treated surfaces have the capacity to down-regulate pro-inflammatory cytokines compared to not treated ones, with presence of M2c macrophages and expression of TGF-β1 after 4 days of culture. However, even though SLM NT surfaces up-regulated pro-inflammatory cytokines, such surfaces may also be good candidates for osteoimmunomodulatory bone implants. The anti-inflammatory cytokine IL-RA was up-regulated and the presence of M2a macrophages was significantly higher compared to cells cultured on SLM PEO surfaces. It can be speculated that the surface porous geometry itself achieved by 3D printing may have important roles in modulating cell/biomaterial interaction, as reported in recent studies for different type of cells [4,5,7].

Bai and Huang recently showed that PEO as titanium surface treatment may be a promising solution in order to develop a new generation of multifunctional bone implants [11,46]. In this study, macrophage response to 3D printed and biofunctionalized titanium implants was evaluated, showing that both implant structure geometry and surface modification had the capacity to modulate macrophage response in terms of polarization. However, knowledge about macrophage response is still limited and the mechanism through which M1 and M2 macrophages influence recruitment and differentiation of bone-forming cells is still poorly understood [62]. In addition to this, protein secretion and gene expression were analysed after 4 days of culture, only considering factors released and expressed at one specific time point. Gene expression and cytokine analysis at different time points is needed in order to have an overview of the factors released by macrophages over the entire culture period.

4.2 Cytotoxicity of Ag NPs

During PEO treatment, Ti-6Al-4V implants containing silver were synthesized by dispersing Ag NPs into the electrolyte at a concentration of 3.0 g/L. Silver is widely used as antimicrobial agent and according to this type of implants, antibacterial activity against *staphylococcus aureus* was previously demonstrated [9]. One of the mechanisms through which Ag nanoparticles exert antimicrobial activity is the release of Ag^+ [63]. For these specific 3D printed PEO-treated surfaces, the Ag^+ release kinetics was previously tested by inductively coupled plasma (ICP); Ag ions were released from the PEO-treated Ti-6Al-4V surfaces up to 28 days, with a higher release rate during the first 3-4 days [9].

In order to assess effects of such ion release on human macrophage polarization, a transwells culture between implants and cells was performed. According to IL-6, TNF-α and CCL18 secretion, no significant difference was found between the experimental groups investigated showing that Ag^+ release did not have an effect on macrophages polarization in the model investigated.

In order to investigate the role of titanium modified surface in human macrophages polarization, cells were cultured directly on the surfaces up to 4 days. Protein secretion, gene expression, cell viability and morphology was evaluated. However, when macrophages were cultured directly on SLM PEO + Ag implants, the concentration of IL-6 and CCL18 in cell supernatant was undetectable after 4 days of culture, for all different 5 donors investigated. This trend was confirmed by gene expression analysis; cells cultured on surfaces containing Ag NPs expressed low/undetectable values of the genes under investigation. Furthermore, low amount of DNA was found for cells cultured on SLM PEO + Ag group, indicating that the number of cells on Ag-bearing surfaces was considerable lower in comparison with cells cultured on the other surfaces investigated. However, SEM images showed a considerable amount of cells on SLM PEO + Ag surfaces. The cells attached uniformly along the surface, but they presented a more rounded shape compared to cells attached to the other types of surfaces and they were smaller in dimensions. This may be attributed to cell apoptosis, since cell shrinkage during this death cell process has been already demonstrated [64]. The hypothesis was confirmed by a live/dead assay, which showed that all macrophages attached to SLM PEO + Ag implants were dead, whereas cells were found alive when cultured on the other types of implants. Nevertheless, Ag NPs did not have cytotoxic effects on hMSCs showing that in this culture model, surface Ag NPs concentration had cytotoxic effects were macrophage-specific.

Silver nanoparticles have been shown to kill bacterial cells, regardless the type of bacteria strain [65]. Furthermore, Li *et al.* [66] proposed three different antimicrobial mechanisms of Ag NPs:

- Alteration of bacteria membrane properties by adhesion of nanoparticles;
- Bacteria DNA damage due to penetration of Ag NPs inside the cell;
- Degradation of Ag NPs into Ag^+ ions that interact with proteins present in cell membrane, leading to compromised functionalities.

Ag NP effects on cells and microbes have been investigated in *in vitro* studies, which demonstrated that such nanoparticles are responsible for cell apoptosis, free radical production and membrane rupture [67]. Another mechanism through which surfaces containing Ag NPs may exert antimicrobial activity is the generation of reactive oxygen species (ROS) [68], which can cause oxidative stresses in macrophages resulting in cytotoxic effects [69–71]. Thus, according to literature, Ag ion release, ROS production and cell mitochondrial damage seem to be the most common and important pathways through which Ag NPs exert toxic effects on cells. However, knowledge about the interaction of these mechanisms is still limited. The results reported in this research are in line with previous *in vitro* studies, which show that macrophages, compared to other cell type, are more sensitive to the toxic effects of Ag NPs. Particles uptake and ROS production was shown to be higher in macrophages compared to epithelial, hepatic and neuronal cells [72]. Macrophages are phagocytic cells, and Internalization of Ag NPs may be explained by the uptake of the particles through scavenger receptors, present on cell wall. Ag NPs, once entered cell membrane, may degrade releasing silver ions, which may lead to induction of oxidative stress due to free radical production. This may result in mitochondrial damage, inducing apoptotic cell death (**Figure 32**). However, such proposed mechanism was evaluated in the presence of free Ag NPs, while in the present studies the particles are incorporated into the implant oxide layer.

As previously stated, in this work silver ions did not induce cell death when released from transwell, suggesting that cell death is dependent on macrophage contact with Ag NPs rather than on ion release from the surface.

Comparison between the biological data from different studies is difficult because of the high variety in NPs sizes, stabilizing surfaces and particle shapes. Furthermore, Ag NPs effects on cells were shown to be dependent on their size, concentration and exposure time [73]. Thus, further investigation including different time points and concentration of Ag NPs in PEO electrolyte is needed.

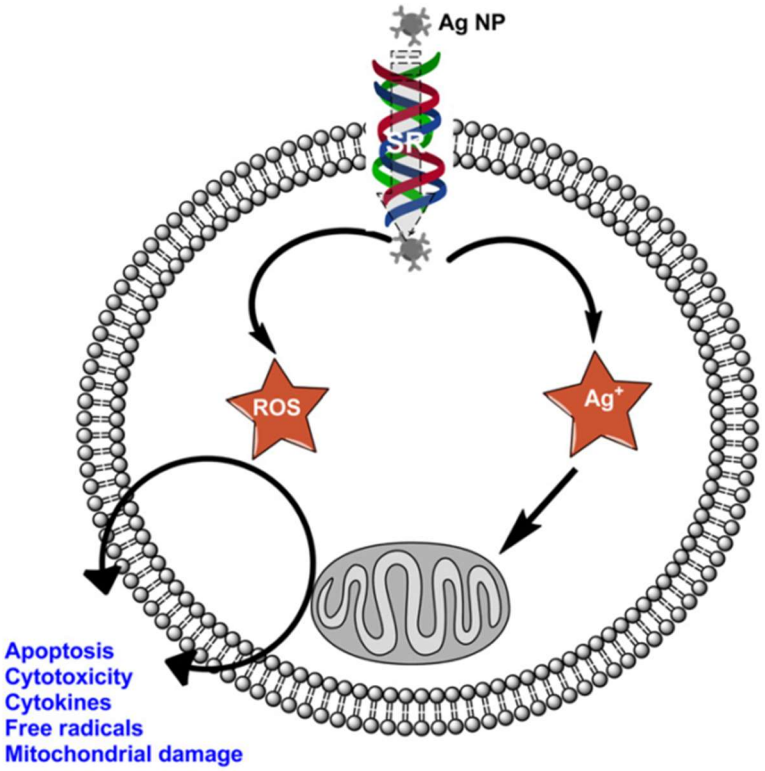

Figure 32: Mechanism through which Ag NPs induce cell apoptosis and mitochondrial damage, as explained by *Singh et al.* [67].

4.3 Towards a new generation of osteoimmunomodulatory bone implants

Bone implant surfaces should be biofunctionalized taking into account three different surface properties:

- Anti-bacterial property;
- Capacity to modulate macrophage inflammatory response;
- Ability to promote bone formation.

With this aim, multifunctional surfaces were synthesized and the macrophage response was evaluated. Macrophages have the capacity to recruit MSCs, and the wound healing as well as bone formation at implant interface is influenced by macrophage/MSC cross-talk [62]. Bone implant surface properties influence macrophage response [21] and they may also influence macrophage/MSC interaction. Using a co-culture model of MCM and hMSCs, migration of MSCs in the presence of factors released from macrophages was investigated. The MCM obtained culturing macrophages on SLM implants enhanced the MSCs migration compared to medium containing FBS only, without factors secreted by macrophages. The assay was performed with cells obtained from one human donor, and future investigation is needed to show the reproducibility of these results. Nevertheless, the very important role of macrophages cultured on SLM implants in recruiting hMSCs was shown.

4.4 Recommendations for future work

Based on the results obtained from this research, the PEO treated surfaces showed promising properties in modulating macrophage response. However, the present research can be further expanded. Further studies should consider to investigate the following aspects:

- Additional characterization of PEO-treated surfaces in order to quantify surface roughness and wettability since these properties are known to modulate macrophage response.
- In order to investigate if the cytotoxic effects on macrophages are concentration-dependent, SLM PEO + Ag implants should be synthesized with different concentrations of Ag NPs.
- Investigation and quantification of the Ag^{+} ion release from SLM PEO + Ag implants. From these data, a relationship between the ion released and the median lethal dose (LD50) for human macrophages can be drawn.
- Culture of human macrophages on SLM implants pre-coated with plasma proteins, in order to have a more accurate reproduction of the *in vivo* situation.
- In order to have an overview of macrophage polarization over the entire culture period, secreted pro- and anti-inflammatory factors at different time points should be investigated.
- In order to evaluate if the SLM surfaces have the capacity to down-regulate macrophage pro-inflammatory secretion, culture cells in a pro-inflammatory environment, by adding LPS to the culture medium.
- Repetition of the MSC migration assay in response to macrophage-conditioned medium in order to test its reproducibility. In addition to this, macrophage secreted factors that are responsible for MSC recruitment should be investigated.
- Development a co-culture system between macrophages and MSCs in the presence of SLM implants in order to investigate their cross-talk during new bone formation. This may be achieved investigating the MSC osteogenic factor expression while co-cultured with macrophages. Furthermore, the effects of macrophages cultured on not treated and PEO-treated surfaces on MSC osteogenic differentiation should be investigated.
- Test of the 3D printed surface-modified Ti-6Al-4V implants in *ex vivo* and *in vivo* models.

5. Conclusions

In order to investigate human macrophage polarization in response to modified 3D printed Ti-6Al-4V bone implants, such implants were modified by plasma electrolytic oxidation (PEO), technique used to generate oxide layers on metal substrates. Multifunctional surfaces presenting interconnected micro- and nano-porosity were successfully synthesized. TiO_2 coatings containing silver nanoparticles (Ag NPs) were also generated, since these surfaces were previously shown to have increased antimicrobial activity. After having characterized the modified Ti-6Al-4V surfaces by SEM and EDS analysis, human macrophage response in terms of morphology, viability and polarization as well as viability of hMSCs were investigated in the presence of such surfaces after 4 days of culture. Finally, effects of MCM on MSCs migration were evaluated.

Not treated surfaces up-regulated the expression of macrophage pro-inflammatory cytokines compared to PEO-treated surfaces. With regard to anti-inflammatory cytokine secretion, both surfaces were found to enhance some of the M2 macrophage markers investigated. Cells cultured on SLM PEO surfaces expressed higher levels of CD163, M2c macrophage marker, while cells cultured on SLM NT surfaces expressed higher levels of CD206, M2a macrophage marker. Thus, not only implant surface modification obtained by PEO, but also the controlled porous geometry achieved by additive manufacturing, may have beneficial roles in modulating human macrophage response. On the other hand, SLM PEO + Ag surfaces were found to be cytotoxic for human macrophages when cultured on such surfaces, while the surface Ag ion release did not have any effect on cells in terms of polarization in the transwell culture. Furthermore, SLM PEO + Ag surfaces were found not cytotoxic for hMSCs cultured on implants under the same conditions, suggesting that macrophages were more sensitive to the presence of Ag NPs on the surface compared to the other type of cell. Furthermore, the important role of macrophages cultured on implants on MSC migration was shown. Based on these data, the Ti-6Al-4V surfaces investigated can be considered promising for the conception and development of multifunctional bone implants.

List of abbreviations

CCL18	Chemokine (c-c motif) ligand 18
CD-14, 163, 206	Cluster of differentiation 14, 163, 206
EDS	Energy dispersive X-ray spectroscopy
ELISA	Enzyme-linked immunosorbent assay
FBS	Fetal bovine serum
GAPDH	Glyceraldehyde-3-phosphate dehydrogenase
GCs	Glucocorticoids
HA	Hydroxyapatite
HPRT-1	Hypoxanthine phosphoribosyltransferase 1
IAI	Implant associated infection
IL-1β, 4, 6, 10, 12, 13, 23	Interleukin-1beta, 4, 6, 10, 12, 13, 23
IL-1RA	Interleukin 1 receptor antagonist
LG	Low glucose
LPS	Lipopolysaccharides
M1	Pro-inflammatory macrophage
M2	Anti-inflammatory macrophage
MACS	Magnetic-activated cell sorting
MAO	Micro-arc oxidation
MCM	Macrophage-conditioned medium
MRSA	Methicillin-resistant *Staphylococcus aureus*
MSC	Mesenchymal stem cells
NP	Nano particle
NT	Not-treated
PBS	Phosphate buffered saline
PEO	Plasma electrolytic oxidation
PFA	Paraformaldehyde
ROS	Reactive oxygen species
SEM	Scanning electron microscopy
SLM	Selective laser melting
TGF-β	Transforming growth factor-beta
TNF-α	Tumor necrosis factor-alpha
VEGF	Vascular endothelial growth factor
XRD	X-ray diffraction

REFERENCES

1. McCracken, M. Dental Implant Materials: Commercially Pure Titanium and Titanium Alloys. *J. Prosthodont.* **8,** 40–43 (1999).

2. Long, M. & Rack, H. J. Titanium alloys in total joint replacement—a materials science perspective. *Biomaterials* **19,** 1621–1639 (1998).

3. Raphel, J., Holodniy, M., Goodman, S. B. & Heilshorn, S. C. Multifunctional coatings to simultaneously promote osseointegration and prevent infection of orthopaedic implants. *Biomaterials* **84,** 301–314 (2016).

4. Zadpoor, A. A. Bone tissue regeneration: the role of scaffold geometry. *Biomater. Sci.* **3,** 231–245 (2015).

5. Ahmadi, S. M. *et al.* Additively Manufactured Open-Cell Porous Biomaterials Made from Six Different Space-Filling Unit Cells: The Mechanical and Morphological Properties. *Mater. (Basel, Switzerland)* **8,** 1871–1896 (2015).

6. Bose, S., Robertson, S. F. & Bandyopadhyay, A. Surface modification of biomaterials and biomedical devices using additive manufacturing. *Acta Biomater.* **66,** 6–22 (2018).

7. Bose, S., Ke, D., Sahasrabudhe, H., Bandyopadhyay, A. & Keck, ⇑ W M. Additive manufacturing of biomaterials. *Prog. Mater. Sci.* **93,** 45–111 (2018).

8. Pałka, K. & Pokrowiecki, R. Porous Titanium Implants: A Review; Porous Titanium Implants: A Review. doi:10.1002/adem.201700648

9. van Hengel, I. A. J. *et al.* Selective laser melting porous metallic implants with immobilized silver nanoparticles kill and prevent biofilm formation by methicillin-resistant Staphylococcus aureus. *Biomaterials* **140,** 1–15 (2017).

10. Yao, S. *et al.* Antibacterial activity and inflammation inhibition of ZnO nanoparticles embedded TiO 2 nanotubes.

11. Huang, Q. *et al.* The Cu-containing TiO2coatings with modulatory effects on macrophage polarization and bactericidal capacity prepared by micro-arc oxidation on titanium substrates. *Colloids Surfaces B Biointerfaces* **170,** 242–250 (2018).

12. Chen, Z. *et al.* Osteoimmunomodulation for the development of advanced bone biomaterials. *Materials Today* (2016). doi:10.1016/j.mattod.2015.11.004

13. Franz, S., Rammelt, S., Scharnweber, D. & Simon, J. C. Immune responses to implants - A review of the implications for the design of immunomodulatory biomaterials. *Biomaterials* (2011). doi:10.1016/j.biomaterials.2011.05.078

14. Anderson, J. M., Rodriguez, A. & Chang, D. T. FOREIGN BODY REACTION TO BIOMATERIALS. *Semin Immunol. Semin Immunol* **20,** 86–100 (2008).

15. Sridharan, R., Cameron, A. R., Kelly, D. J., Kearney, C. J. & O'Brien, F. J. Biomaterial based modulation of macrophage polarization: A review and suggested design principles. *Materials Today* (2015). doi:10.1016/j.mattod.2015.01.019

16. Mantovani, A. *et al.* The chemokine system in diverse forms of macrophage activation and polarization. *Trends in Immunology* (2004). doi:10.1016/j.it.2004.09.015

17. Spiller, K. L. *et al.* Differential gene expression in human, murine, and cell line-derived macrophages upon polarization. (2016). doi:10.1016/j.yexcr.2015.10.017

18. Grotenhuis, N., Bayon, Y., Lange, J. F., Van Osch, G. J. V. M. & Bastiaansen-Jenniskens, Y. M. A culture model to analyze the acute biomaterial-dependent reaction of human primary macrophages. *Biochem. Biophys. Res. Commun.* **433,** 115–120 (2013).

19. Stout, R. D. *et al.* Macrophages sequentially change their functional phenotype in response to changes in microenvironmental influences. *J. Immunol.* **175,** 342–9 (2005).

20. Pittenger, M. F. *et al.* Multilineage potential of adult human mesenchymal stem cells. *Science* **284,** 143–7 (1999).

21. Chen, Z., Wu, C. & Xiao, Y. Convergence of Osteoimmunology and Immunomodulation for the Development and Assessment of Bone Biomaterials. in *The Immune Response to Implanted Materials and Devices* 107–124 (Springer International Publishing, 2017). doi:10.1007/978-3-319-45433-7_6

22. Li, Y. *et al.* Formation and in vitro/in vivo performance of 'cortex-like' micro/nano-structured TiO 2 coatings on titanium by micro-arc oxidation. *Mater. Sci. Eng. C* #pagerange# (2018). doi:10.1016/j.msec.2018.02.023

23. Bai, Y. *et al.* Microarc oxidation coating covered Ti implants with micro-scale gouges formed by a multi-step treatment for improving osseointegration. *Mater. Sci. Eng. C* **76,** 908–917 (2017).

24. Echeverry-Rendón, M. *et al.* Modification of titanium alloys surface properties by plasma electrolytic oxidation (PEO) and influence on biological response. *J. Mater. Sci. Mater. Med.* **28,** (2017).

25. Karageorgiou, V. & Kaplan, D. Porosity of 3D biomaterial scaffolds and osteogenesis. *Biomaterials* **26,** 5474–5491 (2005).

26. Taniguchi, N. *et al.* Effect of pore size on bone ingrowth into porous titanium implants fabricated by additive manufacturing: An in vivo experiment. *Mater. Sci. Eng. C* **59,** 690–701 (2016).

27. Jemat, A., Ghazali, M. J., Razali, M. & Otsuka, Y. Surface Modifications and Their Effects on Titanium Dental Implants. doi:10.1155/2015/791725

28. Hadrup, N. & Lam, H. R. Oral toxicity of silver ions, silver nanoparticles and colloidal silver â€“ A review. *Regul. Toxicol. Pharmacol.* **68,** 1–7 (2014).

29. Puleo, D. A. & Huh, W. W. Acute toxicity of metal ions in cultures of osteogenic cells derived from bone marrow stromal cells. *J. Appl. Biomater.* **6,** 109–116 (1995).

30. Fahy, N. *et al.* Human osteoarthritic synovium impacts chondrogenic differentiation of mesenchymal stem cells via macrophage polarization state. *Osteoarthr. Cartil.* **22,** 1167–1175 (2014).

31. Isolation of mononuclear cells.

32. MP 03224 LIVE/DEAD ® Viability/Cytotoxicity Kit Product Information.

33. CyQUANT® Cell Proliferation Assay Kit. (2006).

34. Fisher Scientific -, T. TRIzol Reagent User Guide - Pub. no. MAN0001271 - Rev. A.0.

35. Farrell, R. E. cDNA Synthesis. doi:10.1016/B978-0-12-374727-3.00017-6

36. Knuth, C. A. *et al.* Isolating Pediatric Mesenchymal Stem Cells with Enhanced Expansion and Differentiation Capabilities. *Tissue Eng. Part C Methods* **24,** 313–321 (2018).

37. Necula, B. S., Apachitei, I., Tichelaar, F. D., Fratila-Apachitei, L. E. & Duszczyk, J. An electron microscopical study on the growth of TiO 2 –Ag antibacterial coatings on Ti6Al7Nb biomedical alloy. (2011). doi:10.1016/j.actbio.2011.02.037

38. Necula, B. S. *et al.* In vitro cytotoxicity evaluation of porous TiO2-Ag antibacterial coatings for human fetal osteoblasts. *Acta Biomater.* **8,** 4191–4197 (2012).

39. Hotchkiss, K. M. *et al.* Titanium surface characteristics, including topography and wettability, alter macrophage activation. *Acta Biomater.* (2016). doi:10.1016/j.actbio.2015.12.003

40. Lee, S. *et al.* Analysis on migration and activation of live macrophages on transparent flat and nanostructured titanium. *Acta Biomater.* (2011). doi:10.1016/j.actbio.2011.01.006

41. Saraste, A. & Pulkki, K. Morphologic and biochemical hallmarks of apoptosis.

42. Kaneshiro, S. *et al.* IL-6 negatively regulates osteoblast differentiation through the SHP2/MEK2 and SHP2/Akt2 pathways in vitro. *J. Bone Miner. Metab.* **32,** 378–392 (2014).

43. GALLUCCI, R. M. *et al.* Impaired cutaneous wound healing in interleukin-6–deficient and immunosuppressed mice. *FASEB J.* **14,** 2525–2531 (2000).

44. Jilka, R. L. *et al.* Increased Osteoclast Development After Estrogen Loss: Mediation by Interleukin-6. *Science* **257,** 88–91

45. Rees, P. A., Greaves, N. S., Baguneid, M. & Bayat, A. Chemokines in Wound Healing and as Potential Therapeutic Targets for Reducing Cutaneous Scarring. doi:10.1089/wound.2014.0568

46. Bai, L. *et al.* A multifaceted coating on titanium dictates osteoimmunomodulation and osteo/angio-genesis towards ameliorative osseointegration. *Biomaterials* (2018). doi:10.1016/j.biomaterials.2018.02.010

47. Tan, J. *et al.* Nano-topographic titanium modulates macrophage response in vitro and in an implant-associated rat infection model. doi:10.1039/c6ra22667a

48. Hamlet, S. & Ivanovski, S. Inflammatory cytokine response to titanium chemical composition and nanoscale calcium phosphate surface modification. *Acta Biomater.* (2011). doi:10.1016/j.actbio.2011.01.032

49. Rydén, L. *et al.* Early inflammatory response in soft tissues induced by thin calcium phosphates. *J. Biomed. Mater. Res. - Part A* **101 A,** 2712–2717 (2013).

50. Nie, B., Ao, H., Zhou, J., Tang, T. & Yue, B. Biofunctionalization of titanium with bacitracin immobilizationshows potential for anti-bacteria, osteogenesis and reduction ofmacrophage inflammation. *Colloids Surfaces B Biointerfaces* (2016). doi:10.1016/j.colsurfb.2016.05.089

51. Wang, Y., Xu, D., Liu, Y., Zhang, R. & Lu, L. The Effect of Tumor Necrosis Factor-α at Different Concentrations on Osteogenetic Differentiation of Bone Marrow Mesenchymal Stem Cells. *J. Craniofac. Surg.* **26,** 2081–2085 (2015).

52. Omar, O. M. *et al.* The correlation between gene expression of proinflammatory markers and bone formation during osseointegration with titanium implants. (2011). doi:10.1016/j.biomaterials.2010.09.011

53. Clark, R. A. F. Overview and General Considerations of Wound Repair. in *The Molecular and Cellular Biology of Wound Repair* 3–33 (Springer US, 1998). doi:10.1007/978-1-4615-1795-5_1

54. Frost, A., Jonsson, K. B., Nilsson, O. & Ljunggren, Ö. Inflammatory cytokines regulate proliferation of cultured human osteoblasts. *Acta Orthop. Scand.* **68,** 91–96 (1997).

55. Lachman, L. B. Human interleukin 1: purification and properties. *Fed. Proc.* **42,** 2639–45 (1983).

56. Gu, Q., Yang, H. & Shi, Q. Macrophages and bone inflammation. *Journal of Orthopaedic Translation* (2017). doi:10.1016/j.jot.2017.05.002

57. Sridharan, R., Cameron, A. R., Kelly, D. J., Kearney, C. J. & O'Brien, F. J. Biomaterial based modulation of macrophage polarization: A review and suggested design principles. *Materials Today* **18,** (2015).

58. Mosser, D. M. & Edwards, J. P. Exploring the full spectrum of macrophage activation. doi:10.1038/nri2448

59. Hamidzadeh, K., Christensen, S. M., Dalby, E., Chandrasekaran, P. & Mosser, D. M. Macrophages and the Recovery from Acute and Chronic Inflammation. doi:10.1146/annurev-physiol-022516-034348

60. Christian Gomes Moura Priscilla Barbosa Ferreira Soares Maria Aparecida de Souza, C. & Zanetta-Barbosa, D. Effect of titanium surface on secretion of IL1β and TGFβ1 by mononuclear cells. *Implant Dent. Braz Oral Res* **50025,** 500–5 (2011).

61. Champagne, C. M., Takebe, J., Offenbacher, S. & Cooper, L. F. Macrophage cell lines produce osteoinductive signals that include bone morphogenetic protein-2. *Bone* **30,** 26–31 (2002).

62. Pajarinen, J. *et al.* Mesenchymal stem cell-macrophage crosstalk and bone healing. (2017). doi:10.1016/j.biomaterials.2017.12.025

63. Feng, Q. L. *et al.* A mechanistic study of the antibacterial effect of silver ions on Escherichia coli and Staphylococcus aureus. *J. Biomed. Mater. Res.* **52,** 662–8 (2000).

64. Saraste, A. & Pulkki, K. Morphologic and biochemical hallmarks of apoptosis. *Cardiovasc. Res.* **45,** 528–537 (2000).

65. Reidy, B., Haase, A., Luch, A., Dawson, K. A. & Lynch, I. Mechanisms of silver nanoparticle release, transformation and toxicity: A critical review of current knowledge and recommendations for future studies and applications. *Materials (Basel).* **6,** 2295–2350 (2013).

66. Li, Q. *et al.* Antimicrobial nanomaterials for water disinfection and microbial control: Potential applications and implications. *Water Res.* **42,** 4591–4602 (2008).

67. Singh, R. P. & Ramarao, P. Cellular uptake, intracellular trafficking and cytotoxicity of silver nanoparticles. *Toxicol. Lett.* **213,** 249–259 (2012).

68. Park, H.-J. *et al.* Silver-ion-mediated reactive oxygen species generation affecting bactericidal activity. (2008). doi:10.1016/j.watres.2008.12.002

69. Foldbjerg, R. *et al.* PVP-coated silver nanoparticles and silver ions induce reactive oxygen species, apoptosis and necrosis in THP-1 monocytes. *Toxicol. Lett.* **190,** 156–162 (2009).

70. Suresh, A. K. *et al.* Cytotoxicity Induced by Engineered Silver Nanocrystallites Is Dependent on Surface Coatings and Cell Types. *Langmuir* **28,** 2727–2735 (2012).

71. Haase, A. *et al.* Toxicity of silver nanoparticles in human macrophages: uptake, intracellular distribution and cellular responses. *J. Phys. Conf. Ser.* **304,** 12030 (2011).

72. Zhang, X.-F., Shen, W., Gurunathan, S. & Sivakov, V. Molecular Sciences Silver Nanoparticle-Mediated Cellular Responses in Various Cell Lines: An in Vitro Model. doi:10.3390/ijms17101603

73. Wang, G., Wan, Y. & Liu, Z. Incorporation of antibacterial ions on the micro/nanostructured surface and its effects on the corrosion behavior of titanium. *Mater. Lett.* **216,** 303–305 (2018).